Constitutively active signaling of MDA5 in Treg cells causes apoptosis of Treg cells and results in autoimmune diseases

Lee Sumin

Table of contents

ABSTRACT

MDA5 is the critical viral RNA sensor for the induction of innate antiviral responses. A missense mutation, MDA5 G821S, was identified in mouse with severe autoimmune phenotypes. G821S substitution causes conformational change of MDA5 protein and confers constitutive signaling without viral RNA. Thus, MDA5 G821S is a gain-of-function mutation and causes constitutive production of antiviral cytokines including type I IFN (IFN-I) and contributes to the pathology. Recently, human genome analyses revealed that gain-of-function mutations of MDA5 cause autoimmune diseases, including Aicardi-Goutières Syndrome (AGS) and Singleton-Merten Syndrome (SMS). Because these diseases are commonly triggered by constitutive production of IFN-I, these are collectively termed as interferonopathy. However, the involvement of Treg cells in the pathogenesis of MDA5 G821S interferonopathy remains unclear. This study aimed to delineate the mechanism between the expression of constitutively active MDA5 in Treg cells and autoimmune diseases. To address this question, mice expressing MDA5 G821S in Treg cells were generated (Treg G821S mice). Treg G821S mice showed a reduction of peripheral Treg cell number due to elevated apoptosis and resulted in scurfy-like phenotypes, including lupus-like nephritis and high lethality. Interestingly, the number of activated Tregs was significantly reduced in AGS patients, suggesting Treg abnormality is a common mechanism for human and mouse interferonopathies. Furthermore, adaptive transfer of wild-type Treg cells into the mice with systemic expression of MDA5 G821S, improved their autoimmune symptoms and lethality. Taken together, this study demonstrates that constitutively active MDA5-mediated signaling disturbs the homeostatic function and activation of Tregs and may contribute to Because MDA5G821S results in constitutive activation of acquired immune responses, the

applicant aimed to elucidate the role of Treg cells in the autoimmune phenotypes. The applicant made mice expressing MDA5 G821S in a Treg-specific manner (Treg G821S mice) and analyzed for Treg population and Treg functions. Treg G821S mice showed a reduction of peripheral Treg cell numbers due to elevated apoptosis. Treg cells from Treg G821S mice failed to suppress in an experimental colitis model, suggesting that G821S disturbs the function of Treg. Treg G821S mice exhibits lupus-like nephritis and high lethality. Examination of Treg G821S mice revealed inflammation in lung, small intestine, colon and kidney, as well as production of auto-antibodies. These were consistent with the results that activated Treg is reduced in AGS patients. Furthermore, adaptive transfer of wild-type Treg cells into systemic G821S mice ameliorated the autoimmune phenotypes and survival. In summary, this study demonstrates that constitutively active MDA5-mediated signaling in Treg cells disturbs Treg cell functions, thereby contributing to the pathology of interferonopathy.

ABBREVIATIONS

ADAR1	Adenosine deaminase acting on RNA
AGS	Aicardi-Goutières syndrome
APCs	Antigen-presenting cells
CTLA-4	Cytotoxic T lymphocyte associated protein 4
DCs	Dendritic cells
ENU	N-ethyl-N-nitorosourea
Foxp3	Forkhead box P3
GATA3	GATA binding protein 3
IFN-I	Type I interferon
IFNAR1	Interferon alpha and beta receptor subunit 1
IFNGS	Type I IFN-inducible gene signatures
IL-4	Interleukin 4
IL-10	Interleukin 10
IL-17	Interleukin 17
IPS-1	IFN-β promoter stimulator 1
IRF 3	Interferon regulatory factor 3
IRF 7	Interferon regulatory factor 7
ISGs	IFN-stimulated genes
LGP2	Laboratory of genetics and physiology 2
MAVS	Mitochondrial antiviral signaling protein
MDA5	Melanoma differentiation-association protein 5
MHC class I	Major histocompatibility complex class I
MHC class II	Major histocompatibility complex class II
NF-κB	Nuclear factor-κb
Nrp-1	Neuropilin-1
PRRs	Pattern recognition receptors
RA	Rheumatoid arthritis
RIG-I	Retinoic acid-inducible gene I
RLRs	RIG-I-like receptors

RNASEH2A	Ribonuclease h2 subunit a
RNASEH2B	Ribonuclease h2 subunit b
RNASEH2C	Ribonuclease h2 subunit c
RORγt	Retinoid orphan receptor gamma t
SAMHD1	SAM domain and HD domain1
SLE	Systemic lupus erythematosus
SMS	Singleton-Merten syndrome
TCR	T cell receptor
T-bet	T-box transcription factor TBX21
TGF-β	Transforming growth factor beta
Th1	T-helper 1
Th2	T-helper 2
Th17	T-helper 17
Tregs	Regulatory T cells
TREX1	Three prime repair exonuclease 1

Chapter 1

Introduction

1-1 Immune system

The immune system has evolved a variety of biological defense mechanisms to combat infection with pathogenic microorganisms or invaders, such as fungi, parasites, bacteria, and viruses in vertebrates, including humans. The immune system consists of two major mechanisms: innate immunity and adaptive immunity. As the initial line of defense, the innate immune response causes cells to identify and inhibit pathogens through pattern recognition receptors (PRRs). They also respond immediately to infection but lack the cellular memory for pathogens [2]. The adaptive immune response, regulated by the innate immune cells, contributes to the activation of T cells and B cells to eliminate the invaders. In addition, the adaptive immune response is slow but causes T and B cells to form persistent memories of pathogens. These two systems safeguard the host against a variety of invaders [3].

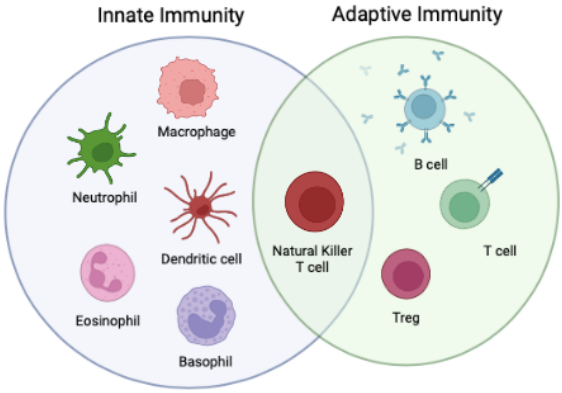

Illustration 1. Cells of the innate and adaptive immune systems

During the innate immune response, phagocytes such as neutrophils, eosinophils, macrophages, basophils, and dendritic cells are actively involved in destroying pathogens. In order to notify adaptive immune system cells, they display the foreign antigen on their cell membrane after engulfing the problematic cell. The adaptive immune system, which is comprised of immune cells like B cells and T cells that are developed to identify and combat that pathogen, is in charge of immune reactions that are antigen-specific. NK cells are considered a component of the innate immune system, although they also work effectively with the adaptive immune system. This illustration is with BioRender.com.

1-2 The role of RIG-I like receptors in the innate immunity

PRRs play an important role in the defense mechanisms of the innate immune system. It has been shown that retinoic acid-inducible gene-I (RIG-I)-like receptors (RLRs), including RIG-I, MDA5, and laboratory of genetics and physiology 2 (LGP2), are critical PRRs for sensing viral RNAs [4] and inducing Type I interferon (IFN-I) and pro-inflammatory cytokines [5]. RIG-I and MDA5 are typical PRRs with a signaling transduction domain, whereas LGP2 is thought to be a regulator of RIG-I- and MDA5-mediated signals [6]. When viral RNAs are detected, RIG-I and MDA5 interact with the mitochondrial antiviral signaling protein (MAVS, also known as IPS1), which recruits the nuclear factor-κB (NF-κB) and interferon regulatory factor 3 and 7 (IRF3/7) to activate them [7-10]. As a result of this process, many pro-inflammatory cytokines/chemokines and antiviral genes, including IFN and IFN-stimulated genes (ISGs), are highly induced. This system plays an essential role in suppressing viral reproduction and transmission.

1-3 Type I IFN involvement in autoimmune disease

IFN-I, an important cytokine, is produced by innate immune cells and also induces the activation of adaptive immune cells. Beyond their critical functions in antiviral defense, IFN-I now understood to be play a major role in autoimmune diseases, such as systemic lupus erythematosus (SLE). Patients with autoimmune diseases have disease-specific pathophysiologies and clinical symptoms, Among the autoimmune diseases, some are linked to aberrant production of IFN-I and/or type I IFN-inducible gene signatures (IFNGS) in their serum or tissues, as genetical abnormalities, and are collectively called as Type I interferonopathy [11–13]. Typical type I

interferonopathies include Aicardi-Goutières syndrome (AGS), SLE, rheumatoid arthritis (RA), and Singleton-Merten syndrome (SMS).

1-4 Aicardi–Goutières syndrome (AGS)

Aicardi-Goutières syndrome (AGS) is a rare type I interferonopathy caused by mutations in the genes encoding several proteins. AGS results from both loss-of -function and gain-of-function mutations. Loss-of-function mutation are identified in three prime repair exonuclease 1 (TREX1-AGS1), ribonuclease H2 subunit A/B/C (RNASEH2A- AGS4, RNASEH2B- AGS2, RNASEH2C-AGS3), deoxynucleoside triphoshate triphosphohydrolase and ribonuclease SAM domain and HD domain1 (SAMHD1-AGS5), adenosine deaminase acting on RNA (ADAR1- AGS6) genes. Gain-of-function mutations are identified in double-stranded RNA cytosolic sensor IFN-inducted helicase C domain containing protein 1 (IFIH1; or MDA5- AGS7) genes [16,17]. Patients with the AGS-associated mutations on these genes exhibit higher expression levels of IFN-I in their blood, which usually causes encephalopathy syndrome, severe inflammation, and leukoencephalopathy [14,15].

1-5 Gain-of-function MDA5 G821S mutant

MDA5 consists of a DExD/H-type RNA helicase domain, a C-terminal domain for viral RNA recognition, and two caspase recruitment domains (CARDs) at the N-terminus for signal transduction. Analysis of the protein structure using atomic force microscopy revealed that wild-type MDA5 (MDA5 WT) forms an open-ring structure with connecting linkers between the three domains. MDA5 binds to double-stranded RNA and triggers ATP hydrolysis in the conserved helicase domains. The ATPase activity of MDA5 WT was extremely low in the absence of dsRNA but significantly

increased in the presence of dsRNA-mimic polyI:C. Unlike RIG-I, which preferentially senses short dsRNA with 5'ppp, MDA5 has a higher affinity to bind with long dsRNA. Upon activation, MDA5 monomers oligomerize along the dsRNA to induce its filamentation, which is thought to be essential for conducting downstream signaling with mitochondrial MAVS. Activation of MAVS then triggers IRF-3-mediated production of type I interferon and cytokines [44].

In 2014, our research group published a study of mice that spontaneously developed SLE-like phenotypes by inducing gene mutations. For the gene mutations, we used N-ethyl-N-nitrosourea (ENU), which functions as a chemical mutagen capable of inducing mutations with a high frequency. As a result of the genetic analysis, it was found that the gene responsible for the phenotype was located in the 1.04 Mb region of the second chromosome. Genomic DNA sequencing for all genes in this region confirmed that the mutation was identified in exon 13 of *Ifih1*, encoding mouse MDA5, with a single base substitution (G replaced by A) at the 2461st G from the 5' end (Illustration 2). This single base substitution changes the 821st glycine (G) to serine (S) (G821S mutation). Further analyses revealed that the mutated MDA5 functions as a gain-of-function mutant. Furthermore, in contrast to MDA5 WT, MDA5 G821S was observed to form a closed ring structure under the AFM analysis. And MDA5 G821S showed no elevated ATPase activities even in the presence of poly I:C. Therefore, the conformational changes rather than the sensitivity to endogenous RNA ligands contribute to the constitutive activity of MDA5 G821S [44].

MDA5$^{G821S/+}$ mice showed significant developmental delay and high mortality, and developed nephritis at 6 weeks of age. Immunoglobulin deposition was observed in the glomeruli, and concentrations of various immunoglobulins such as IgG, IgA, and IgM, anti-nuclear antibodies, and anti-double-stranded DNA antibodies were

significantly increased in the serum. In addition, the gene expression of inflammatory cytokines and chemokines, including *IFN-β*, *IL-6, CXCL10, ISG56,* and *TNF-α,* in the kidney was significantly increased compared to that of WT mice. Using flow cytometry analysis of the effect of active MDA5 on immune cells using splenocytes from MDA5$^{G821/+}$ mice, it was confirmed that innate immune cells such as dendritic cells and macrophages were significantly increased and activated. Activation of dendritic cells and macrophages was also confirmed to induce a decrease in naive T cells, an increase in effector T cells [44].

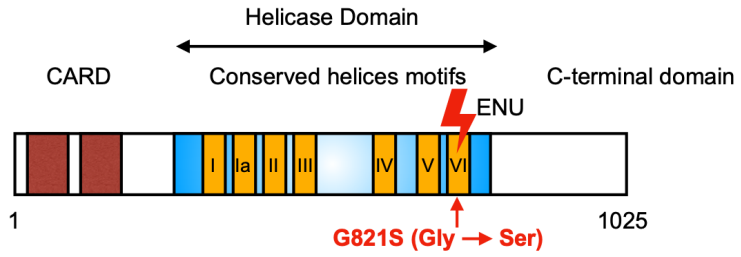

Funabiki, M et al. *Immunity* 2014

Illustration 2. Structure of the mutant MDA5 G821S

ENU was used to induce mutations in the helicase domain of MDA5. Glycine at position 821 is substituted with serine. This mutation leads to continuous activation of MDA5, leading to overproduction of IFN-I and inflammatory cytokines.

1-6 Innate control of adaptive immunity: T cells

Innate immune cells, such as dendritic cells (DCs) or other APCs, engulf and are resultantly activated by invasive pathogens, viruses, or vaccines. Activated innate immune cells then migrate to the lymph nodes and use MHC class I or II, known as the major histocompatibility complex, to expose pathogenic antigens to T lymphocytes [18-20]. Specialized T-cell receptors (TCR) allow T lymphocytes recognize the particular antigen/receptor presentation [21]. TCR bound to MHC class I or II induces T cell activation and differentiation. As described above, various signals from the innate immune system play key roles in leading to the activation of immune cells in the adaptive immune system.

1-7 CD4 Th cell subsets.

T cells can only recognize an antigen when it is presented by MHC molecules. CD8+ cytotoxic T cells and CD4+ helper T cells identify antigens presented in the context of MHC class I and MHC class II molecules, respectively. The effector cell that the CD4+ T helper cells will develop into is determined by a variety of signals that are generated during the process of recognition of the pathogen.

1-8 Differentiation of helper T cell

Naive TH0 T lymphocytes are specific for antigen and are stimulated for proliferation upon contact with APCs that express MHC class II/peptide complexes. TH0 cells can be propelled along one of many differentiation pathways depending on the kind of APCs and the cytokines presented at the site of antigen contact. In addition to the conventional T-helper 1 (Th1) and T-helper 2 (Th2) subsets, other subsets have also been identified, such as T-helper 17 (Th17) and regulatory T (Tregs) cells. Each of

these subgroups has a distinct profile of cytokines. Th1 cells mediate immune responses against viruses and intracellular bacteria [22, 23]. However, the majority of organ-specific autoimmune diseases are thought to be caused by abnormal Th1 cell activation. Th1 cells activate macrophages by secreting IFN-γ, IL-2, and tumor necrosis factor (TNF)-beta and they are responsible for phagocytosis-dependent protective responses and cell-mediated immunity [22, 23]. Th2 cells are essential for parasite immunity and have been shown to be implicated in inflammatory pathologies associated with allergies and asthma [23–25]. Th2 cells secrete IL-4, IL-5, IL-10, and IL-13 to promote eosinophil activation and trigger a phagocytic response that inhibits macrophage activities [23–26]. Th17 cells are essential for the defense against extracellular bacteria and fungi and have been shown to be implicated in autoimmune diseases such as RA and SLE. Th17 cells secrete IL-17a, IL-17f, and IL-23 to promote neutrophils [27–30]. The differentiation of helper T cells is depicted in Illustration 3.

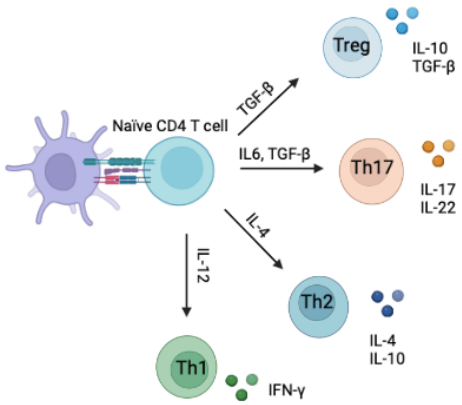

Illustration 3. CD4+ T cell subset differentiation.

Differentiation of Th1 cells relies on transcription factors such as T-bet to release IFN-γ, IL-2 and TNF-β to provide protection against viruses and intracellular bacteria. Differentiation of Th2 cells relies on transcription factors such as Gata3 that induce the secretion of IL-4, IL-5, IL-10, and IL-13 to protect against parasites. TGF-β is crucial in the differentiation of Tregs and Th17 cells. TGF-β alone causes naive CD4+ T cells to differentiate into Foxp3+ Tregs that secrete IL-10 and TGF-β; however, TGF-β and IL-6 together induce Th17 cell differentiation. Th17 cells induce up-regulation of RORγt, followed by the production of Th17 cytokines, including IL-17 and IL-23 [28]. Th17 cells are essential for both inflammatory autoimmune disorders and host defense against infections. This illustration is with BioRender.com.

1-9 Tregs and their roles in human diseases

Tregs play an important role in maintaining homeostasis and self-tolerance by suppressing the pro-inflammatory activity of APCs and cytokines [31, 32]. Tregs are traditionally identified by the expression of CD25, CTLA-4, Nrp-1, and Foxp3 (see Illustration 4) [33, 34, 35]. Foxp3 is a transcription factor required for regulating differentiation, development, and the suppressive function of Tregs [36]. Genetic defects in Foxp3 cause the loss of Treg cells, which disrupts the control of inflammatory effector T cell activation, leading to lethal autoimmune disorders in humans and mice [38, 39]. The deficiency of Tregs can lead to inflammatory disorders and autoimmune diseases such as RA, SLE, and inflammatory bowel disease (IBD). However, little is known about the causes of Treg dysfunction.

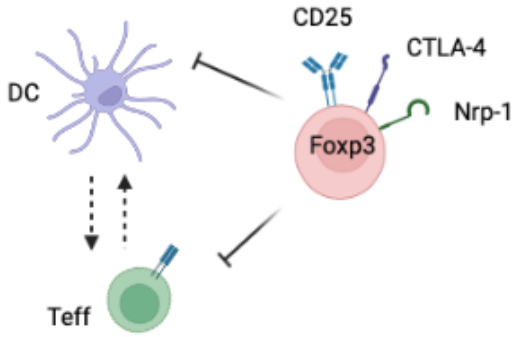

Illustration 4. Mechanisms of Treg suppression.

Tregs can indirectly reduce T eff by reducing the expression of costimulatory molecules on DCs through CTLA-4. This illustration is with BioRender.com.

1-10 Purpose of my research

Recent studies have demonstrated the impact of type I IFN on Treg function using several experimental models of autoimmunity, viral infection, and cancer. One study demonstrated that in an autoimmune disease mouse model, chronic IFN signature due to the loss of DNA exonuclease Trex1 inhibits the proliferation and activation of Tregs. However, this inhibition does not contribute to the pathogenesis of inflammatory diseases [39]. In contrast, another study showed that IFNAR signaling in Tregs also down-regulates the suppressive activity of Tregs, which is beneficial for antiviral and anti-tumor responses [40]. Type I IFNs are clearly shown to be potent down-regulators of Treg function; however, the underlying mechanisms, including effective timing, extent of type I IFN expression, as well as the general or case-specific contribution of the reduced Treg activity to the pathogenesis, virus load, and tumorigenesis, remain to be clarified. Our research group has previously reported a chronic IFN signature and various autoimmune disease in mice with a constitutively active mutant of the viral sensor MDA5 (designated as MDA5 G821S/+ mice) [41-43], which had been obtained by ENU mutagenesis. I herein investigated the role of MDA5 signaling on Treg cells by using Foxp3-Cre to generate MDA5 G821S knock-in mice, in which MDA5 is constitutively active only in Treg cells. In the mice with conditionally activated MDA5 on Treg cells, I detected autoimmune disease-like phenotypes characterized by nephritis, and Treg deficiency. Furthermore, I report that effector Treg cells are decreased in AGS patients, similar to the Foxp3 mutant mouse model. These results suggest that MDA5 signaling acts on the homeostasis, survival, and function of Treg cells.

Chapter 2

Materials and methods

2-1 PBMC from healthy donors and AGS patients

The peripheral blood mononuclear cells (PBMCs) samples were obtained from healthy donors and AGS patients with the approval of the Medical Ethics Committee of Kyoto University School of Medicine. The study protocols were performed in accordance with the principles contained within the Declaration of Helsinki. PBMCs were isolated using Ficoll-paque gradients (GE Healthcare).

2-2 Mice

The Foxp3 tm4 $^{YFP\text{-}icre}$ mice were purchased from the Jackson Laboratory. Foxp3$^{cre/-}$ MDA5 G821S$^{flox/wt}$ male and Foxp3$^{cre/cre}$ MDA5 G821S$^{flox/wt}$ female with C57B/6J background were proliferated by in vitro fertilization of Foxp3$^{cre/-}$ MDA5 G821S$^{flox/wt}$ sperm × Foxp3$^{cre/wt}$ MDA5 G821S$^{wt/wt}$ female ovum. MDA5$^{G821S/+}$ mice with a DBA/2 background were propagated by in vitro fertilization of MDA5$^{G821S/+}$ sperm and DBA/2JJcl female ovum. Rag2$^{-/-}$ and Ifnar1$^{-/-}$ mice were purchased from B&K Universal. All mice were maintained in the Kyoto University's specific pathogen free facility and handled in accordance with the institutional guidelines for animal care and use.

2-3 Generation of the MDA5 G821S $^{flox/flox}$ mice

I generated a targeting construct containing a loxP, exon 13 fragment, stop codon, poly A and PGK-Neo cassette with loxP sites, followed by linking the mutant exon 13 G821S (Illustration 5). Sequences of missense mutations in MDA5 exon 13 were amplified by polymerase chain reaction (PCR) and then inserted into the above construct. The linearized targeting vector was then transduced into murine hybrid embryonic stem (ES) cells by electroporation. ES cells were tested for successful recombination by Northern blotting. Chimeric mice were bred with C57BL/6 mice to generate germ line transmission (MDA5 G821S$^{flox/+}$ mice). To generate Foxp3 cell-specific knock-in mice, MDA5 G821S$^{flox/+}$ mice were crossed with Foxp3 tm4 $^{YFP\text{-}icre}$ mice to generate mutation MDA5 G821S$^{flox/wt}$ Foxp3$^{cre/-}$ mice. The mutation of MDA5 G821S cDNA was confirmed by PCR analysis using the following primers:

F 5′-GCTTTACTGTCCAAGTCACTGCTC-3′,

R 5′-GGAGGCTTTGTGTTTGAATCTGG-3′.

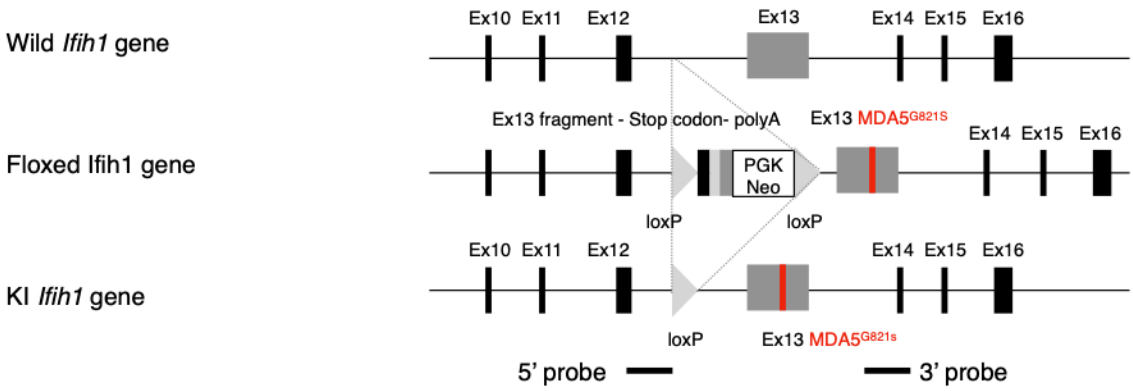

Illustration 5. Schematic of MDA5 G821S targeting construct. Diagrams show wild-type allele, targeting allele, floxed allele (MDA5 G821S flox knock-in)

2-4 Preparation of single-cell suspensions

Single-cell suspensions from mesenteric lymph nodes and spleen were obtained by passing the organs through 70μm nylon screens in phosphate buffered saline (PBS) containing 10% FBS (Gibco) and 2mM EDTA (Nacalai Tesque). Red blood cells were eliminated with ACK lysis buffer (Gibco). After removing Peyer's patches in the small intestine, the intestine was cut longitudinally, then washed thoroughly in cold PBS and incubated in shaker for 20 min at 37°C in RPMI-1640 containing 3% FBS, 100mM DTT (Sigma) and 0.5mM EDTA. After washing several times, the intestine was cut into small tissues then digested for 23 min at 37°C with 0.5mg/ml DNase (Sigma) and 1mM/ml Liberase TL (Roche) in RPMI-1640. Single cells were obtained through 70μm nylon screens in PBS containing 10% FBS and 2mM EDTA .

2-5 Cell sorting and adoptive transfer of regulatory T cells

To sort $CD4^+YFP^+$ cells from Foxp3-gs and Foxp3-wt for qPCR, single cells were stained with anti-CD4 (APC, RM4-5, BioLegend), $CD4^+YFP^+$ Treg cells were sorted using BD FACSAriaIII. The purity of the sorted population was >90%. To sort $CD4^+CD25^{hi}$ T cell subpopulation from WT mice for adoptive transfer experiments, splenocytes were first separated through negative selection using CD4 MicroBeads (Miltenyi Biotech). $CD4^+$T cells were then stained with APC-anti-mouse CD4 (RM4-5, BioLegend) and PE-anti-mouse CD25 (PC61, BD bioscience). $CD4^+CD25^{hi}$ Treg cells were sorted using BD FACSAriaIII (purity>80%). $MDA5^{G821S/+}$ recipients were initially injected with $CD4^+CD25^{hi}$ Treg ($5x10^5$ cells) intraperitoneally, followed by $CD4^+CD25^{hi}$ Treg ($1x10^5$ cells) once a week until death. *Rag2*$^{-/-}$ recipients were injected intravenously (IV) with $CD4^+CD25^-$ Tn ($5x10^5$ cells) and $CD4^+CD25^{hi}$ Treg ($5x10^5$ cells) and allowed to reconstitute for 5-6 weeks.

2-6 Flow Cytometry analysis

For surface staining, cells were resuspended in 100μl of FACS buffer (10% FBS and 2mM EDTA in PBS) and incubated with the respective antibodies for 15 min at 4°C in the dark. Cells were washed twice with 1ml of FACS buffer. For intracellular staining of Foxp3, after the surface staining, cells were incubated in Transcription Factor Fixation and Permeabilization solution (Invitrogen) for 30 min at RT and stained with anti-Human FoxP3 (PCH101, BioLegend) or anti-mouse FoxP3 (MF-14, BioLegend) in Foxp3/Transcription Factor Staining Buffer for 30 min at 4°C (Invitrogen). For Active Caspase 3 assays, after the surface staining, cells were incubated in BD Cytofix/Cytoperm (PE-Active Caspase 3 Apoptosis kit, BD Science) for 20 min at 4°C and stained with Caspase 3 (PE-Active Caspase 3 Apoptosis kit, BD Science) and GFP (FM264G, BioLegend) antibody in BD Perm/Wash buffer for 30 min in the dark. For cell viability analysis, after the surface staining, cells were incubated with Annexin V (BioLegend) and 7ADD (BioLegend) for 15 min at 4°C in Annexin V binding buffer (BioLegend). Data were collected using a BD Biosciences LSRFortessa and analyzed using FlowJo software (Tree Star, Inc).

Antibodies used in flow cytometry were shown in Table 1.

Table 1: Antibody list

	Antibody	Clone	Format	Source
anti-mouse	CD4	RM4-5	APC, PE-Cy7, Pacific Blue	BioLegend
	CD8a	53-6.7	APC	BioLegend
	CD25	PC61	PE, Alexa Fluor 488	BD bioscience
	CD44	IM7	Brilliant Violet 421	BioLegend
	CD62L	MEL-14	PE	BioLegend
	FoxP3	MF-14	APC, PE	BioLegend
anti-Human	CD4	RPA-T4	Pacific Blue	BioLegend
	CD25	BC96	PE	BioLegend
	Foxp3	PCH101	APC	Invitrogen
	CD45RA	HI100	FITC	BioLegend
	Live/Dead		APC-Cy7	Invitrogen
	GFP	FM264G	Alexa Fluor488	BioLegend
	7ADD			BioLegend
	Annexin V		APC	BioLegend
	Caspase-3		PE	BD bioscience

2-7 Quantitative Real-Time PCR

RNA was prepared with the RNAeasy Plus kit (QIAGEN). cDNA was synthesized from RNA using a High-capacity cDNA Reverse Transcription kit (Thermo Scientific). Reverse transcription-PCR was performed in a StepOnePlus Real-Time PCR System (Applied Bio-systems) using the TaqMan Fast Universal PCR Master Mix (Applied Biosystems) or the SYBR Green Real-Time PCR Master Mixes (Applied Biosystems). TaqMan primers for mice *Ifnb1* and *18s rRNA* were purchased from Applied Biosystems. All quantification cycle data were normalized to Gapdh or 18s rRNA and fold changes were calculated by ΔΔ Ct method.

Primer sequences used for real-time PCR were shown in Table 2.

Table 2: Primer list

Gene	Forward primer (5'->3')	Reverse primer (5'->3')
GAPDH	CCCCAGCAAGGACACTGAGCAA	GGGGTCTGGGATGGAAATTGTGAGG
MDA5	GCTGCTAAAGACGGAAATCG	TCTTGTCGCTGTCATTGAGG
ISG56	ATGGGAGAGAATGCTGATGG	CCCAATGGGTTCTTGATGTC
CXCL-10	GACGGTCCGCTGCAACTG	GCTTCCCTATGGCCCTCATT
IL-6	CATGTTCTGGGAAATCGTGG	GTACTCCAGGTAGCTATGGTAC
BIM	GCCAAGCAACCTTCTGATGT	CTGTCTTGCGGTTCTGTCTG
NOXA	GGAGTGCACCGGACATAACT	TTGAGCACTCGTCCTTCA
Bad	CGAAGGAGCGATGAGTT	CCCACCAGGACTGGATAATG-3
PUMA (BBC3)	TGCTCTTCTTGTCTCCGCCG	CATAGAGCCACATGCGAGCG
Mcl-1	AAGCCAGCAGCACATTTCTGATGCC	GTAATGGTCCATGTTTTCAAAGATG
Bcl-xL	ACCAGCCACAGTCATGCCCGTCAGG	GTAGTGAATGAACTCTTTCGGGAATGG
Bcl-2	GGTCTTCAGAGAGACAGCCAGGAGAAATC	GTGGTGGAGGAACTCTTCAGGGATG

2-8 Immunofluorescence and Histological analysis

Tissues were fixed in 4% paraformaldehyde solution (Nacalai Tesque) and embedded in paraffin. Paraffin sections were cut into sections (3 μm) and stained with Hematoxylin-Eosin (Tissue-Tek). Histological analysis was performed on a BZ-X800E microscope (KEYENCE).

Immunofluorescence staining of IgG in kidney tissues was performed. For staining, paraffin-embedded sections of 2-3μm thickness were prepared. After deparaffinization and rehydration, samples were rinsed with PBS and blocked with Protein Block (Dako Japan, Tokyo, Japan), which was followed by incubation with 470 units/ml Proteinase-k (FUJIFILM) at Room Temperature (RT) for 5 minutes. PBS with a 20% concentration of donkey serum (Jackson ImmunoResearch) and 0.05% Triton-X (Sigma) was incubated with the samples at RT for 60 minutes. PBS containing 20% donkey serum, 0.05% Tween-20, Alexa Fluor 647-conjugated donkey anti-mouse IgG antibody (1:500 Jackson ImmunoResearch) and DAPI (1:1000) was incubated with the samples at RT for 60 minutes in the dark. After several washes with PBS, the slides were sealed with Fluoromount-G (Southern Biotech). Immunofluorescence images were captured on a Leica TCS SP8 confocal microscope (Leica).

2-9 Detection of Anti-nuclear Antibodies (ANA)

Serum was diluted 1:20 in PBS for indirect immunofluorescence on fixed L929 cells. The slides were incubated for 60 min at RT, then washed with PBS containing 0.2% Tween-20 for 10 min. The slides were incubated with goat anti-mouse IgG Alexa Fluor 488 (Jackson ImmunoResearch) and DAPI (1:1000) at RT for 20 min. After several washes with PBS, the slides were sealed with Fluoromount-G (Southern Biotech). Immunofluorescence images were captured on a Leica TCS SP8 confocal microscope (Leica).

2-10 Statistical Analysis

Statistical analyses were performed using the GraphPad Prism 9.0 software. Groups of data were compared using a Student's t-test or the ANOVA. Data in bar and dot graphs are means ± SEM. Significance is indicated as follows: *P < 0.05; **P < 0.01; ***P < 0.001; ****P < 0.0001, ns, not significant.

Chapter 3

Results

3.1 Comparison of Foxp3^{+} Treg population in CD4^{+}CD25^{+} cells between wild-type and MDA5$^{G821S/+}$ mice

Our laboratory previously published an article that a gain-of-function MDA5 G821S mutant causes type I interferonopathy in mice [41-43]. However, it is unclear how the constitutive MDA5 signaling regulates the behavior of cells, specifically T cells, to cause autoimmune disease. To determine whether the alteration of T cells occurs in MDA5 mutant mice, I first measured the populations of CD4^{+} and CD8^{+} T cells in the spleen. The percentage of CD8^{+} T cells was not markedly changed, however, a significantly lower percentage and total number of CD4^{+} T cells were observed in the spleen of MDA5$^{G821S/+}$ mice (Figure 1 A, B and C). CD25 expression is an activation marker of CD4^{+} T cells and a surface marker of Tregs. Surprisingly, MDA5$^{G821S/+}$ mice showed an approximately 4-fold increase in the percentage of CD4^{+}CD25^{+} cells compared to WT mice (Figure 1 D). Foxp3, a transcription factor of Treg, plays an essential role in suppressing immune responses activated by both auto-antigens and foreign-antigens [33,44]. To study Tregs in CD4^{+}CD25^{+} cells, I analyzed the expression of Foxp3 in CD4^{+}CD25^{+} cells. Although the amount of Foxp3^{+} Tregs was significantly reduced in MDA5$^{G821S/+}$ mice due to the decreased total number of CD4^{+} T cells, the percentage of Foxp3^{+} population among CD4^{+}CD25^{+} cells was similar to that of WT mice (Figure 1 E and F). These data indicate that systemic activation of MDA5 signaling changes Treg numbers but not the proportion of Foxp3^{+} cells.

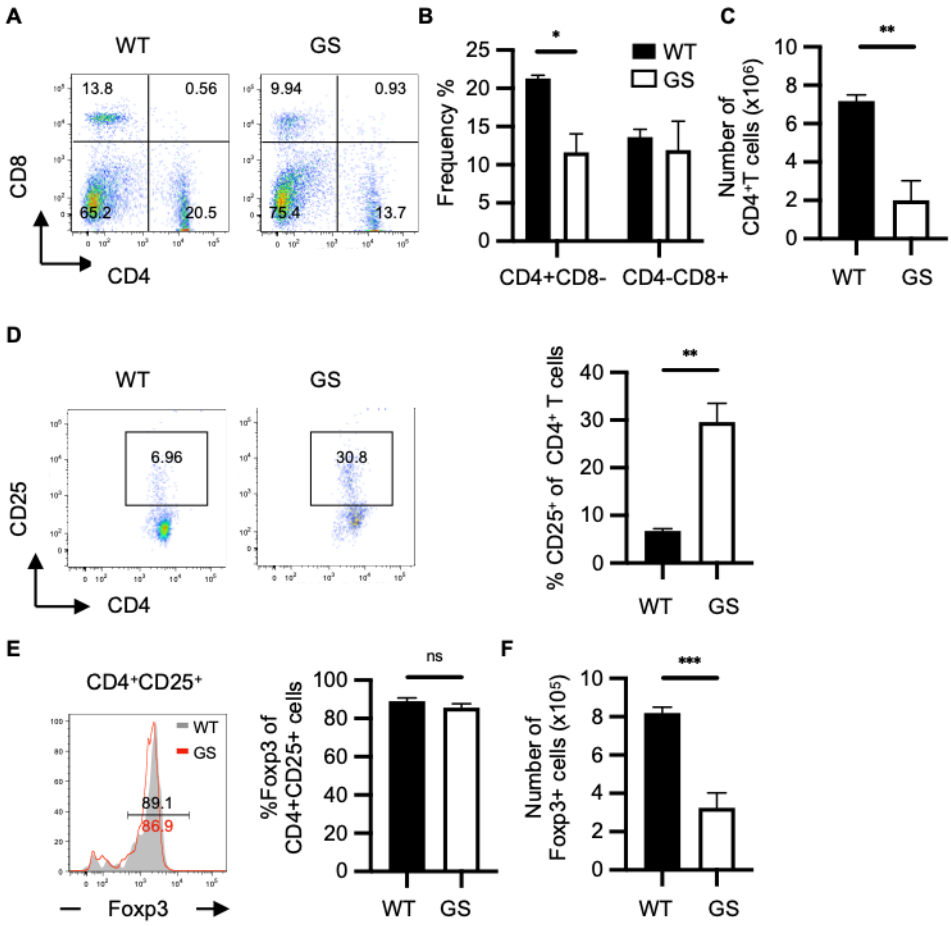

Figure 1 : **Analysis of Treg population and total number in MDA5$^{G821S/+}$ mice.**
(A) Representative flow cytometric analysis of CD4 and CD8 expression of WT or MDA5$^{G821S/+}$ (GS) splenocytes. (B) Statistical analysis of (A) (Each n=3, 10 weeks). (C) Total CD4$^+$ T cell number of WT or GS splenocytes (Each n=3, 10 weeks). (D) Flow cytometric and statistical analysis of CD25 expression of CD4$^+$ T cells of WT or GS splenocytes (wt n=4, GS n=6, 8~10 weeks). (E) Flow cytometric and statistical analysis of Foxp3 expression of WT or GS CD4$^+$CD25$^+$ T cells (Each n=7, 8~10 weeks). (F) Total number of CD4$^+$CD25$^+$Foxp3$^+$ cells. Bar graphs represent the mean ±SEM. Statistical significance was analyzed by one-way ANOVA or unpaired t test. *P ≤ 0.05, **P ≤ 0.01, ***P ≤ 0.001, ****P ≤ 0.0001, ns, not significant.

3.2 Tregs from MDA5$^{G821S/+}$ mice fail to prevent the colitis in *Rag2*$^{-/-}$ mice induced by adoptive transfer of naïve CD4^{+} T cells from WT mice

To investigate if the CD4^{+}CD25^{+} cells in MDA5$^{G821S/+}$ mice retain suppressive function as Tregs, I utilized the experimental colitis model wherein naïve CD4^{+} T cells are transferred into *Rag2*$^{-/-}$ mice [45]. According to this method, adoptive transfer of naïve CD4^{+}CD25^{-} T cells (Tn) into *Rag2*$^{-/-}$ mice results in inflammatory colitis, whereas transferring Tn together with WT CD4^{+}CD25^{+} Tregs can prevent colitis [45]. As shown in (Figure 2 A), I confirmed that *Rag2*$^{-/-}$ mice injected only with Tn from WT mice induced weight loss and colitis development due to the absence of Tregs (green) (Figure 2 B). Furthermore, co-transfer of Tn and CD4^{+}CD25^{+} Tregs from WT mice into *Rag2*$^{-/-}$ mice resulted in weight gain and mice remained asymptomatic, similar to those injected with saline (blue and black) (Figure 2 B). Co-transfer of WT Tn and CD4^{+}CD25^{+} Tregs from MDA5$^{G821S/+}$ mice (red) to Rag2$^{-/-}$ recipients, on the other hand, resulted in clinical signs of colitis, diarrhea, and severe weight loss, similar to mice injected with WT Tn alone (Figure 2 B and C). To examine whether MDA5$^{G821S/+}$ CD4^{+}CD25^{+} Tregs were pathogenic rather than being simply non-functional, I next transferred only CD4^{+}CD25^{+} Tregs from WT or MDA5$^{G821S/+}$ mice to *Rag2*$^{-/-}$ mice (Figure. 2 D). *Rag2*$^{-/-}$ mice transferred with CD4^{+}CD25^{+} Tregs from WT mice were asymptomatic (blue) (Figure. 2 E and F). However, the transfer of CD4^{+}CD25^{+} Tregs from MDA5$^{G821S/+}$ mice induced weight loss and destroyed epithelial tissue (red) (Figure. 2E and F), indicating that Tregs in MDA5$^{G821S/+}$ mice not only lost their suppressive activity, but were also pathogenic as a result of direct signaling of mutant MDA5 and chronic inflammatory environment in MDA5$^{G821S/+}$ mice.

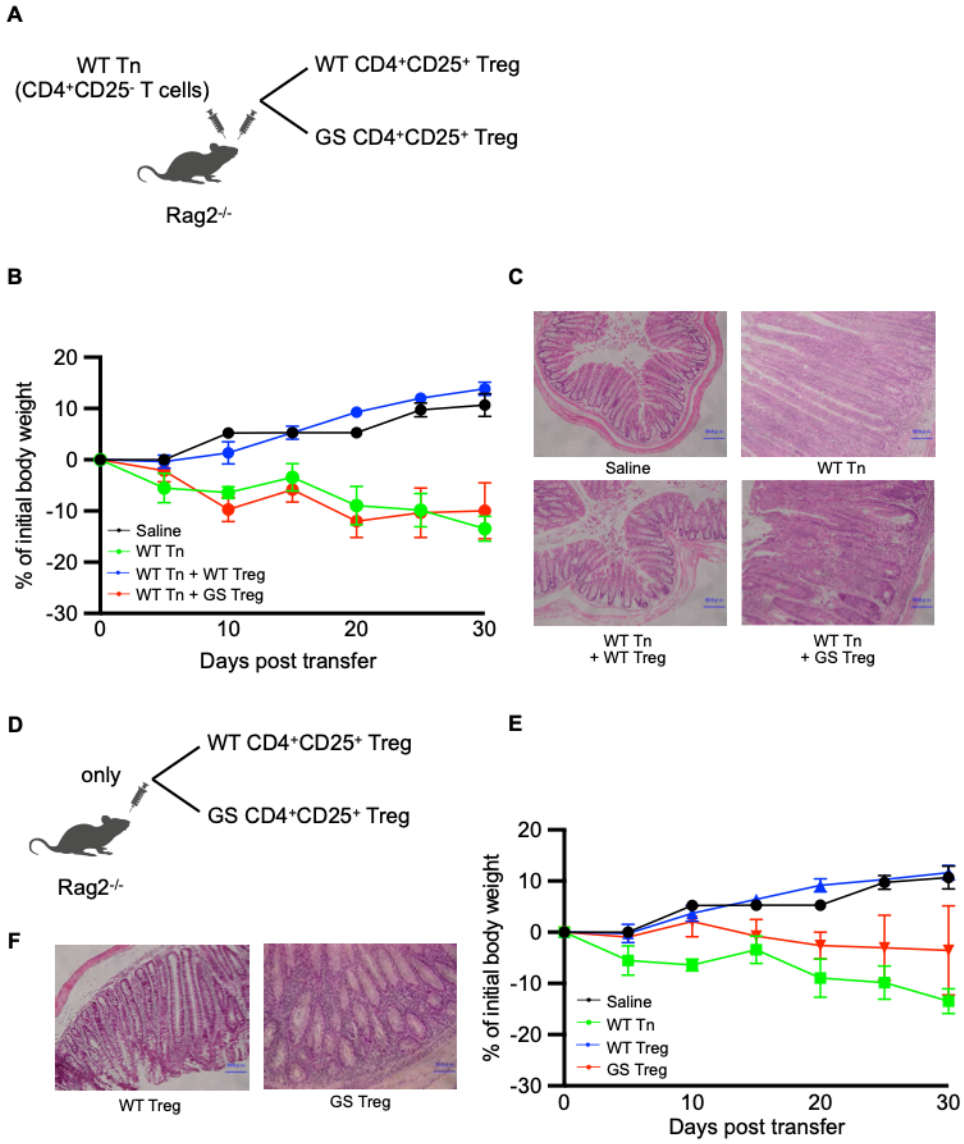

Figure 2. CD4⁺CD25⁺ Tregs from MDA5$^{G821S/+}$ mice fail to prevent weight loss and colitis in *Rag2*$^{-/-}$ mice with adoptive transfer of Tn cells

(A) Diagram of the experimental design. CD4⁺CD25⁻ Tn cells from WT mice were transferred into *Rag2*$^{-/-}$ mice along with CD4⁺CD25⁺ Treg cells from WT or MDA5$^{G821S/+}$ mice. Control mice were injected with saline or Tn from WT mice. (B) Body weight loss curves of *Rag2*$^{-/-}$ recipients. (saline n=3, WT Tn n=4, WT Tn+WT Tregs n=5, WT Tn+ GS Tregs n=5). (C) Representative H&E staining of the colon 30 days after adoptive transfer. Scale bar 50 µm. (D) Diagram of the experimental design. CD4⁺CD25⁺ Treg cells from WT mice or MDA5$^{G821S/+}$ mice. were transferred into *Rag2*$^{-/-}$ mice. (E) Body weight loss curves of *Rag2*$^{-/-}$ recipients. (saline n=3, WT Tn n=4, WT Tregs n=4, GS Tregs n=4). (C) Representative H&E staining of the colon 30 days after adoptive transfer.

3.3 Mice expressing MDA5$^{G821S/+}$ only in the Foxp3+ Treg cells develop systemic lupus erythematosus

To study the effects of MDA5 signaling in Tregs, I specifically exchanged MDA5 for MDA5 $^{G821S/+}$ in Foxp3^{+}Treg cells of mice using the Cre/loxp system [46]. I crossed MDA5 $^{G821S/+}$ Floxed mice with Foxp3 $^{YFP\text{-}Cre}$ mice, in which Foxp3 Tregs can be distinguished by yellow fluorescent protein. Remarkably, Foxp3$^{cre/+}$ MDA5$^{G821S/+}$ (Foxp3-gs) mice exhibited growth retardation compared to Foxp3$^{cre/+}$ MDA5$^{WT/+}$ (Foxp3-wt) mice (Figure 3 A and B). Furthermore, it has been shown that about 50% of the mutant mice died within 8 weeks of birth (Figure 3 C). This phenotype is similar to that of the scurfy mouse strain with the Foxp3 mutation. Next, the histological analysis revealed that massive leukocyte infiltration and chronic inflammation of the small intestine, colon, lung, and kidney occurred in Foxp3-gs mice (Figure 3 D). The presence of nephritis in mutant mice implies that severe SLE was induced [47]. Indeed, IgG deposition was detected in the glomeruli, similar to nephritis in Foxp3-gs mice (Figure 3 E). In addition, anti-nuclear antibody (ANA) was that induce nephritis detected in the serum of Foxp3-gs mice (Figure 3 F). As expected, the expression levels of inflammatory cytokines such as *Isg56*, *IFN-β* and *IL-6* were significantly upregulated in the kidneys of Foxp3-gs mice (Figure 3 G). Thus, chronic activation of MDA5 in Foxp3+ Treg cells leads to the overactivation of the immune system and the lethal systemic autoimmune phenotype.

Figure 3.

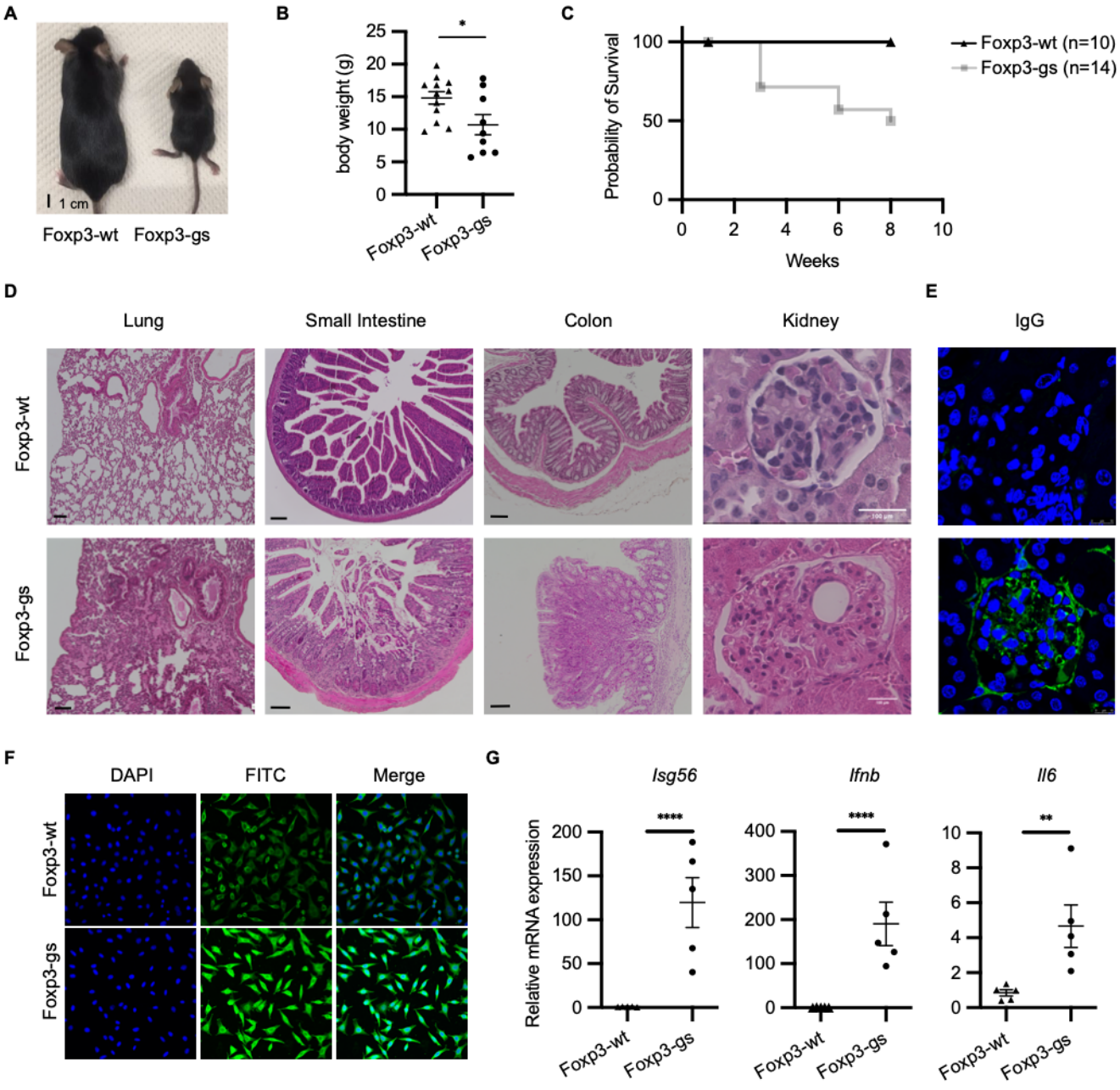

Figure 3. Mice expressing MDA5$^{G821S/+}$ only in the Foxp3^{+} Treg cells develop systemic lupus erythematous

(A) Representative Foxp3-gs and Foxp3-wt mice picture (8 weeks). (B) Body weight of Foxp3-gs mice and Foxp3-wt mice (Foxp3-wt n=12 Foxp3-gs n=9, 4 weeks) (C) Survival curve of Foxp3-gs and Foxp3-wt mice (wt n=10, gs n=14). (D) Representative H&E stained lung, small intestine, colon and kidney. Scale bar 100μm. (E) Representative Immunoglobulin depositions (IgG) of kidney. Scale bar 100μm. (F) Production of ANA in Foxp3-gs and Foxp-wt sera. (G) Expression of *ISG56*, *IFN-b, IL-6* and *Cxcl10* in kidney were analyzed by qPCR (Each n = 5, 8 weeks). Each symbol indicates an individual mouse. Data represent the means ±SEM. Statistical significance was analyzed by two-way ANOVA or Student's t-test. *P ≤ 0.05, **P ≤ 0.01, ***P ≤ 0.001, ****P ≤ 0.0001.

3.4 Foxp3 decrease in activated MDA5$^{G821S/+}$ Treg cells

Given that autoimmune diseases such as SLE or IPEX syndrome are caused by a deficiency of Tregs [48-50], I investigated the populations of $CD4^{+}YPF^{+}$ Treg cells in MDA5 mutant mice. $CD4^{+}YPF^{+}$ Treg cells with significantly reduced proportion and total number were observed in the spleen and small intestine of Foxp3-gs mice compared to Foxp3-wt mice (Figure 4 A and B); this defect was evident in the small intestine and spleen after 6 months of age but not observed in the thymus, indicating that Treg development was not impaired.

To determine whether mutant MDA5 was linked to the homeostasis of Treg cells, I analyzed the frequency of memory and naive T cells in the spleen. Importantly, similar to CD25 Tregs deficiency in mice, the spleen of Foxp3-gs mice had a drastic increase in the frequency of effector/memory (CD62L-CD44+/CD62+CD44+) CD8+T cells compared to Foxp3-wt mice (Figure 4 C, D, and E). These results indicated that aberrant MDA5 signaling severely impacted Treg homeostasis, resulting in a dramatic increase in effector and memory T cells.

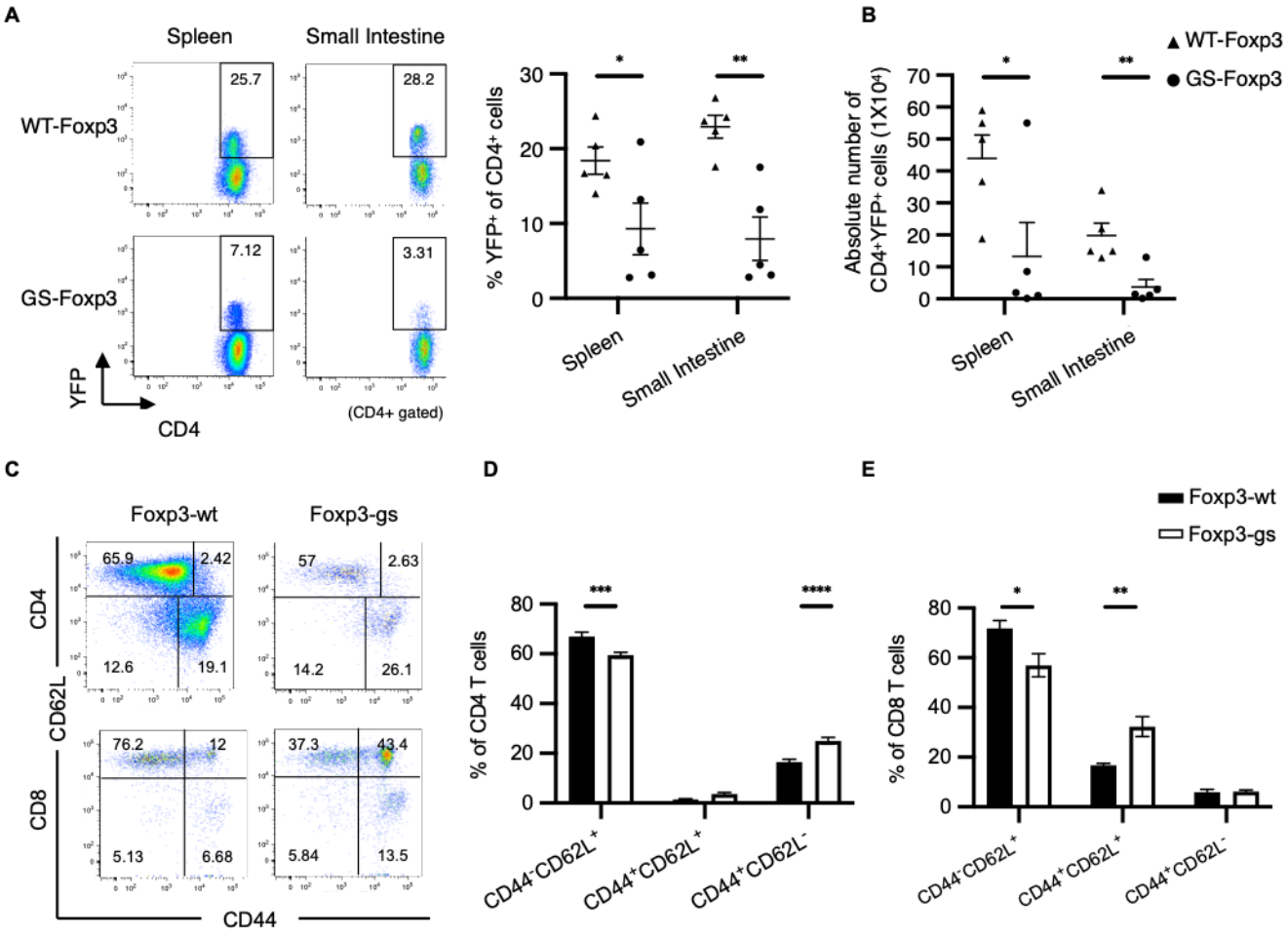

Figure 4. Foxp3 decrease in activated MDA5$^{G821S/+}$ Treg cells

(A) Representative flow cytometric dot plots and (B) percent of CD4$^+$YFP$^+$ Tregs in spleen and small intestine of Foxp3-gs and Foxp3-wt mice (Each n=5, 6~12 months). (C) Representative flow cytometric dot plots and (D and E) frequencies of T cell activation markers CD44 CD62L in CD4$^+$ cells and CD8$^+$ cells from spleen (Foxp3-wt n=5, Foxp3-gs n=8, 8 weeks). CD44$^+$CD62L$^-$ cells are effectors T cells, CD44$^-$CD62L$^+$ cells are naive T cells and CD44$^+$CD62L$^+$ cells are central memory T cells. Each symbol indicates an individual mouse. Data represent the means±SEM. Statistical significance was analyzed by two-way ANOVA or Student's t-test.. *P ≤ 0.05, **P ≤ 0.01, ***P ≤ 0.001, ****P ≤ 0.0001.

3.5 Activated MDA5 induces apoptosis on Foxp3^{+} Treg cells

To explore the cell death of the MDA5 G821S Tregs, I measured annexin V and 7-aminoactinomycin D (7AAD) among CD4+YFP+ Tregs by flow cytometry. I divided them into four subpopulations: AV-/7AAD- live cells, AV+/7AAD- early apoptotic cells, AV-/7AAD+ necrotic cells, and AV+/7AAD+ late apoptotic cells. The results showed that Foxp3-gs mice in MLN and spleen had approximately 3-9 fold higher numbers of apoptotic cells (AV+/7AAD+) than Foxp3-wt mice (Figure 5 A and B). In addition, I analyzed caspase-3 activity in CD4^{+}YPF^{+} Tregs. This data also exhibited approximately 5–10 fold higher rates of apoptosis in Foxp3-gs mice (Figure 5 C and D). To analyze whether the mutant MDA5 induces apoptosis in Tregs, I checked the mRNA expression levels of *MDA5*, *Isg56* and apoptosis genes in MDA5 mutant Tregs. I found that *MDA5* and *Isg56* were highly induced in Tregs (Figure 5 E, F, and G). Furthermore, *Puma* and *Noxa* were also shown to have significantly higher levels than those of anti-apoptotic proteins such as *Bcl-2, Mcl,* and *Bcl-xl* (Figure 5 H). These results suggest that the MDA5 defect induced Treg apoptosis.

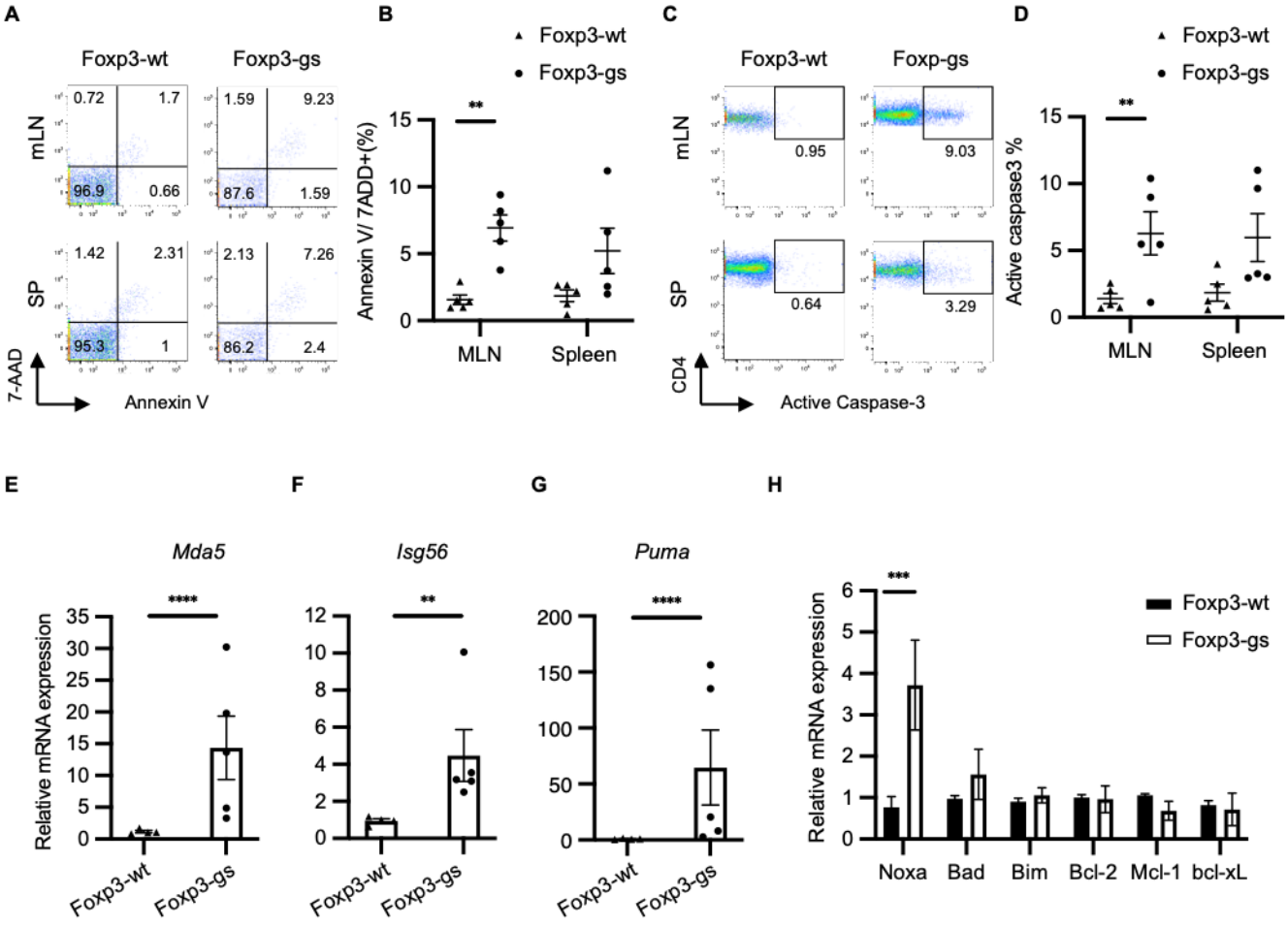

Figure 5. Activated MDA5 induces apoptosis on Foxp3⁺ Treg cells

(A) Representative dot plots and (B) statistical summary of Annexin V/7AAD staining of CD4⁺YFP⁺ Treg cells from spleen and mesenteric lymph nodes of Foxp3-gs and Foxp3-wt mice (each n=5, 8~15 weeks). (C) Representative dot plots and (D) statistical summary of Active Caspase3 staining of CD4⁺YFP⁺ Tregs from spleen and mesenteric lymph nodes of Foxp3-gs and Foxp3-wt mice (each n=5, 8~15 weeks). Expression of *MDA5* (E), *Isg56* (F), *Puma* (G) and total apoptosis gene (H) in CD4⁺YFP⁺ Treg cells purified from mesenteric lymph nodes of Foxp3-wt or Foxp3-gs by BD FACSAria III sorting and analyzed by qPCR (Foxp3-gs n=5, Foxp3-wt n=4, 8~15 weeks). Data represent the means±SEM. Statistical significance was analyzed by two-way ANOVA or Student's t-test.*P ≤ 0.05, **P ≤ 0.01, ***P ≤ 0.001, ****P ≤ 0.0001.

3.6 Type I IFN signaling is required for MDA5-dependent apoptosis in Foxp3$^{cre/+}$ MDA5$^{G821S/+}$ mice

To further investigate the contribution of IFN signaling to the apoptosis of MDA5 mutant Tregs, I inhibited IFNAR signaling by crossing Foxp3$^{cre/+}$ MDA5$^{G821S/+}$ mice with *Ifnar*$^{-/-}$ mice. I found that the CD4^{+}YFP^{+} Treg population of *Ifnar*$^{-/-}$ Foxp3$^{cre/+}$ MDA5$^{G821S/+}$ mice in the spleen and small intestine was fully recovered to Ctr mice level (Figure 6 A and B). Importantly, *Ifnar*$^{-/-}$ Foxp3$^{cre/+}$ MDA5$^{G821S/+}$ mice ameliorated the expression of active caspase-3 in the spleen and mesenteric lymph node in the CD4^{+}YFP^{+} Treg population (Figure 6 C and D). In addition, the expression of *MDA5* and *Puma* in CD4^{+}YPF^{+} Tregs from *Ifnar*$^{-/-}$ Foxp3$^{cre/+}$ MDA5$^{G821S/+}$ mice recovered to WT mice level (Figure 6 E and F). Taken together, these data demonstrated that type I IFN signaling is required for the induction of MDA5- dependent apoptosis in Foxp3$^{cre/+}$ MDA5$^{G821S/+}$ mice.

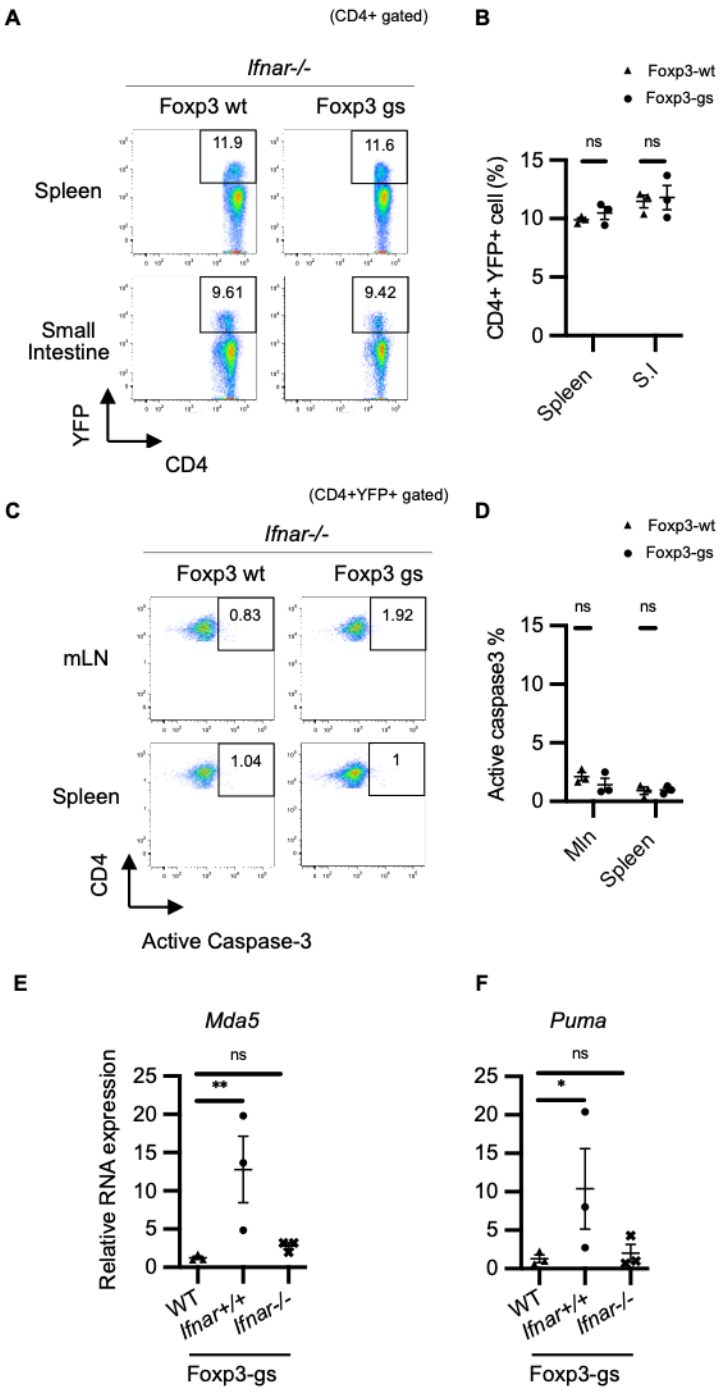

Figure 6. Type I IFN signaling is required for MDA5-dependent apoptosis in Foxp3$^{cre/+}$ MDA5$^{G821S/+}$ mice

(A) Representative flow cytometric dot plots, (B) percent of CD4^{+}YFP^{+} Treg cells within spleen and small intestine of *Ifnar$^{-/-}$Foxp3-gs* and *Ifnar$^{-/-}$Foxp3-wt* mice(Each n=3, 6 months). (C) Representative dot plots and (D) statistical summary of active caspase3 staining of CD4^{+}YFP^{+} Treg cells from spleen and mesenteric lymph nodes of *Ifnar$^{-/-}$Foxp3-gs* and *Ifnar$^{-/-}$Foxp3-wt* mice (Each n=3, 6 months). Expression of MDA5 (E) and Puma (F) in CD4^{+}YFP^{+} Treg cells purified from mesenteric lymph nodes of *Ifnar$^{-/-}$Foxp3-gs* and *Ifnar$^{-/-}$Foxp3-wt* by BD FACSAria III sorting and analyzed by qPCR (Each n=3 6 months). Bar graphs represent the mean ±SEM. Statistical significance was analyzed by two-way ANOVA *P ≤ 0.05, **P ≤ 0.01, ***P ≤ 0.001, ****P ≤ 0.0001, ns, not significant.

3.7 CD4+CD25+ Treg treatment protect MDA5$^{G821S/+}$ mice from death

To analyze whether apoptosis of Tregs induced by activated MDA5 is the major cause of the lethal phenotype in MDA5$^{G821S/+}$ mice *in vivo,* I injected CD4^{+}CD25^{+} Tregs into MDA5$^{G821S/+}$ mice from day 7, as Treg production begins [51]. In this setup, I used systemic MDA5$^{G821S/+}$ mice, which express the mutant MDA5 G821S protein in all cells, not just Treg cells. I found that both MDA5 mice displayed the same rates of apoptosis 3 days after the first injection of PBS or WT-CD4^{+}CD25^{hi} Tregs (Data not shown). MDA5 mice injected with PBS showed an approximately 3-fold decrease in the percentage of CD4^{+}CD25^{+}Foxp3^{+} Tregs compared to WT mice (Figure 7 B). However, injection of CD4^{+}CD25^{+} Tregs from WT mice into MDA5$^{G821S/+}$ increased the percentage of CD4^{+}CD25^{+}Foxp3^{+} Tregs approximately 2-2.5 fold compared to injected PBS-MDA5$^{G821S/+}$mice (Figure 7 B). Furthermore, I found that injection of CD4^{+}CD25^{+} Tregs into MDA5$^{G821S/+}$ mice resulted in weight gain (Figure 7 C). MDA5$^{G821S/+}$ mice treated with WT CD4^{+}CD25^{+} Tregs also exhibited an increased survival rate and attenuated disease symptoms, whereas more than 60% of PBS-treated MDA5$^{G821S/+}$ mice died within 20 days of birth. Despite this, lethality was not completely abrogated in WT CD4^{+}CD25^{+} Treg-injected MDA5$^{G821S/+}$ mice. (Figure 7 D).

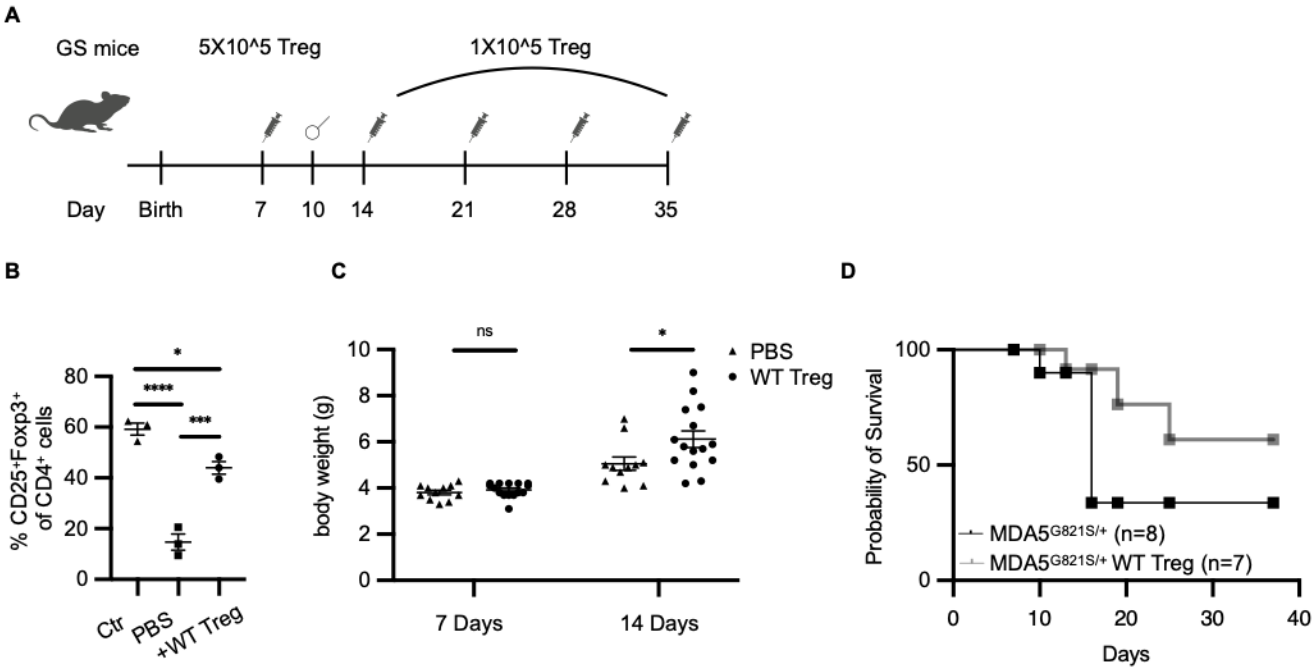

Figure 7. WT CD4^{+}CD25^{+} Treg treatments reverse the lethal phenotype of MDA5$^{G821S/+}$ mice

(A) Diagram of the experimental design. (B) Representative statistical summary of CD4^{+}CD25^{+}Foxp3^{+} cells in the spleen of neonatal MDA5$^{G821S/+}$ mice treated with 5x10^{5} CD4^{+}CD25^{hi} WT Treg cells or PBS i.p injection. MDA5$^{G821S/+}$ mice were injected at days 7 after birth and analyzed at day 10. (C) Body weight graph of neonatal MDA5$^{G821S/+}$ mice treated with 5x10^{5} CD4^{+}CD25^{hi} WT Treg cells or PBS i.p injection. After measuring the body weight of neonatal MDA5$^{G821S/+}$ mice were injection with 5x10^{5} WT Treg cell and again measured body weight after one week. (D) Survival curve of neonatal MDA5$^{G821S/+}$ mice mice treated with CD4^{+}CD25^{hi} WT Treg cells or PBS i.p injection. Neonatal MDA5$^{G821S/+}$ mice were injected with 5x10^{5} CD4^{+}CD25^{hi} WT Treg cells at days 7 after birth. Then one week later, from the second injection, mice were injected with 1x10^{5} CD4^{+}CD25^{hi} WT Treg cells every per week. Data represent the means±SEM. Statistical significance was analyzed by Student's t-test.*P ≤ 0.05, **P ≤ 0.01, ***P ≤ 0.001, ****P ≤ 0.0001, ns, not significant.

3.8 AGS patients has decreased level of activated Treg cells in the peripheral blood

To determine the proportions of different populations of Treg cells in the peripheral blood of the AGS patients, $CD4^+$ T cells in PBMC from healthy donors were stained with CD45RA, a known marker of naive T lymphocytes, and CD25. $CD4^+$ T cells were separated into six subpopulations (Fraction I-VI) [52] and divided into 3 subpopulation based on the degree of Foxp3 expression [53] (Figure 8 A). In particular, these three Treg populations could be clearly defined by the combination of CD25, CD45RA and Foxp3; which were $CD45RA^+$ $CD25^+$ $Foxp3^+$ resting Treg cells (rTreg cells, Fraction I), $CD45RA^-CD25^{++}Foxp3^{++}$ activated Treg cells (aTreg cells, Fraction II) and cytokine-secreting $CD45RA^-CD25^{++}Foxp3^+$ (non Treg cells, Fraction III) nonsuppressive T cells (Figure 8 A) [52-53]. The age-related distribution of Treg subsets showed that healthy child donors had increased resting Tregs compared to healthy adult donors (Figure 8 B). This difference is not seen in other Treg populations and may be the result of decreased production of naive T cells and increased antigens in adult blood due to the thymic erosion, which began at age 20 [54].

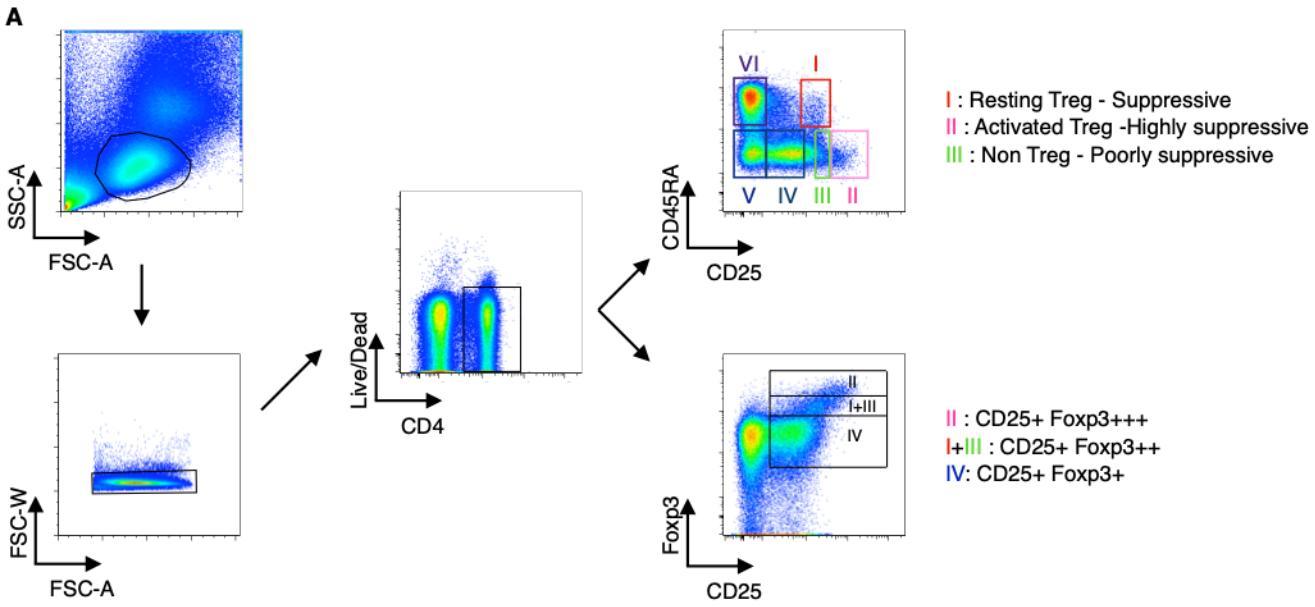

B

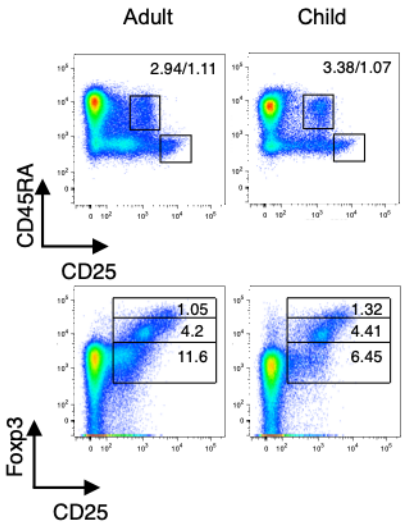

Healthy Donor	Adult	Infant/ Child
Number of individuals	5	6
Age (Years)	20~50	2~18
Activated Treg (t-test vs Adult, means ± SEM)	-	NS -0.1837 ± 0.09780
Resting Treg (t-test vs Adult, means ± SEM)	-	*** 2.050 ± 0.3191
$CD25^{+}Foxp3^{+++}$ (t-test vs Adult, means ± SEM)	-	NS 0.1483 ± 0.07882

Figure 8. Gating strategy for the detection of Treg cells

(A) Phenotypic characterization of $CD4^{+}CD25^{+}$ Treg subset cells. six subset of $CD4^{+}$ T cells are defined by the expression of CD45RA and CD25; $CD45RA^{+}CD25^{+}$ cells (I); $CD45RA^{-}CD25^{++}$ cells (II); $CD45RA^{-}CD25^{+}$ cells (III); $CD45RA^{-}CD25^{+}$ cells (IV); $CD45RA^{-}CD25^{-}$ cells (V); $CD45RA^{+}CD25^{-}$ (VI) cells. The expression of Foxp3 in each fragment show in. Three subset of $CD4^{+}$ T cells are divided by CD25 and Foxp3: $CD25^{+}Foxp3^{++}$ cells (II); $CD25^{+}Foxp3^{+}$ cells (I+III); and $CD25^{+}Foxp3^{-}$ cells (IV). Representative dot plots (B) and statistical summary (Table 1) of PBMC stained for the expression of CD25 and Foxp3 on gated $CD4^{+}$ T cells from healthy adult donors (n=5) and healthy child donors (n=6). Data represent the means±SEM. Statistical significance was analyzed by two-way ANOVA or Student's t-test.*P ≤ 0.05, **P ≤ 0.01, ***P ≤ 0.001, ****P ≤ 0.0001, ns, not significant.

As shown above, in child donors, the frequency of resting Tregs was not dramatically increased by pediatric AGS (Figure 8 B); however, adult AGS patients (Red) have significantly higher resting Treg frequency than the healthy adult donors (Figure 9 A and C). The frequencies of activated Tregs and $CD25^{+}$ $Foxp3^{++}$ among $CD4^{+}$ cells associated with suppressive capacity were not significantly different between healthy child donors and healthy adult donors (Figure 8 B). In contrast, I found evidence for reduced frequencies of activated Tregs (Figure 9A and D) and $CD25^{+}Foxp3^{++}$ (Figure 9B and E) among $CD4^{+}$T cells in both pediatric and adult AGS patients. In addition, the p3 patient (Blue) who was treated with the JAK-inhibitor, which is a competent therapeutic agent for AGS, showed similar results to the frequencies of activated Treg (Figure 9A and D) and $CD25^{+}Foxp3^{++}$ Tregs (Figure 9B and E) from healthy donors. However, in critically ill patients (Red), the frequency of activated Tregs (Figure 9A and D) was remarkably reduced compared to healthy donors. These results suggest that, similar to Foxp3 mutant mice, the population of $CD4^{+}CD25^{+}Foxp3^{+}$ Tregs is significantly reduced in AGS patients. Taken together, this study demonstrates that constitutive MDA5 and type I IFN signaling in Tregs resulted in decreased Treg numbers and ability to maintain homeostatis, which contribute to the induction of various symptoms in cases of interferonopathy.

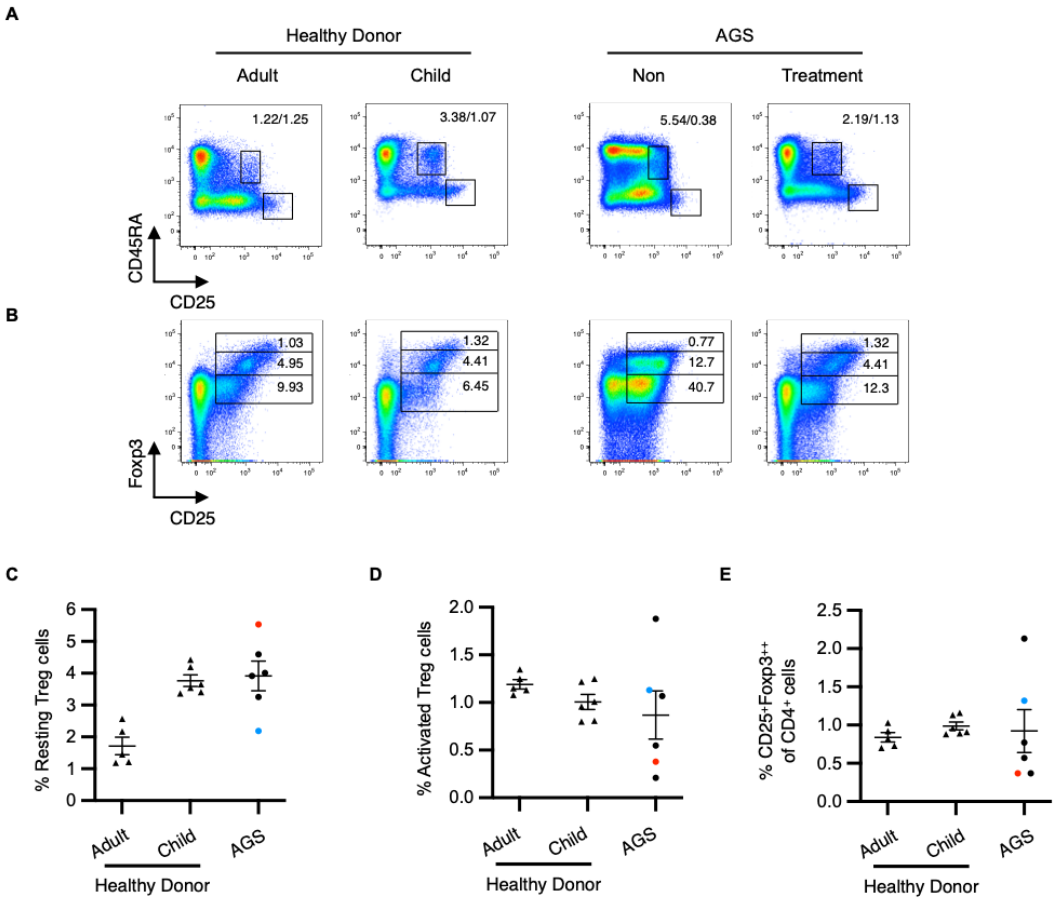

Table 3. Mutations and Interferon score of 6 Aicardi-Goutières syndrome (AGS) patients

Patient	Genotype	Age	Sex	Nucleotide change	Amino acid change	Interferon Score	Treatment	rTreg	a Treg	CD25+ Foxp3++	
P1	MDA5	29	F					adult ** child *	adult ** child *	adult ns child ns	Red
P2	MDA5	25	F	c.2336G>A	p.R779H	150.43	Mycophenolate mofetil	adult ns child ns	adult ** child **	adult *** child ***	
P3	MDA5	16	M	c.1466C>A	p.A489D	25.8	JAK-Inhibitor (Baricitinib)	adult ns child *	adult ns child ns	adult * child ns	Blue
P4	TREX1	5	M	c.52G>A	p.Asp18Asn	11.7064	-	adult * child ns	adult ** child ns	adult * child **	
P5	SAMHD1	15	F	c.428G>A c.1562A>G	p.Arg143His p.Tyr521Cys	74.9395	Prednisolone, Methotrexate	adult * child ns	adult ** child *	adult * child **	
P6	RNASEH2A							adult * child ns	adult ns child ns	adult ns child *	

Figure 9. AGS patients has decreased level of activated Treg cells in the peripheral blood

(A) Representative flow cytometric dot plots of CD45RA+CD25+ T cells within CD4+ T cells in healthy donors, AGS patients. (B) Representative flow cytometric dot plots of CD25+ Foxp3+ Treg cells within CD4+ T cells in healthy donors, AGS patients. (C-E) Statistical summary of PBMC stained for the expression of CD25 and Foxp3 on gated CD4+ T cells from healthy adult donors (n=5) and AGS patients (n=6). (Table1) Mutations and interferon score of 6 Aicardi-Goutières syndrome patients. Data represent the means±SEM. Statistical significance was analyzed by two-way ANOVA or Student's t-test.*P ≤ 0.05, **P ≤ 0.01, ***P ≤ 0.001, ****P ≤ 0.0001, ns, not significant.

Chapter 4

Discussion

Discussion

Mutations in certain genes have been identified as the cause of AGS in a subset of patients. Among these are mutations that lead to the gain-of-function of MDA5, demonstrating the importance of MDA5-dependent type I IFN signaling in the development of disease. Systemic MDA5 G821S/+ mice show constant activation of T cells and innate immune cells such as DCs, macrophages, and NK cells [41-43]. The aberrant activation of these immune cells results in severe autoimmune disease with type I interferonopathy [11-13]. However, the functional analysis of Tregs in AGS patients was not established in previous research.

Treg cells are required for immune homeostasis and the prevention of autoimmune diseases [32]. Here, by using the adoptive transfer colitis model of Rag2-/- mice [45], I demonstrated that Tregs in MDA5 G821S/+ mice have less suppressive activity compared to those in WT mice (Figure 2 A-C) and showed a more pathogenic phenotype (Figure 2 D-E).

To elucidate the role of MDA5 G821S on Treg cells, I generated Foxp3-GS mice that specifically express MDA5 G821S in Treg cells. Treg-specific mutation of MDA5 caused a severe autoimmune disease with scurfy-like phenotypes (Figure 3A). Interestingly, I found that Foxp3-gs mice with severe symptoms showed a Treg deficiency similar to that of scurfy mice (Figure 4A and B), whereas Foxp3-gs mice with mild symptoms showed an increase in the number of Tregs. Furthermore, increased Tregs apparently resulted in a robust induction of active caspase-3 (Figure 5 C and D) and other pro-apoptosis genes such as PUMA and NOXA (Figure 5 E–H). However, the absence of an IFNAR signal in the mutant mice improved the survival rate, and more importantly, the expression of active caspase-3 and other apoptosis

genes in Tregs was restored to a similar level as that in the wt mice (Figure 6). Furthermore, I demonstrated that injection of WT-CD4+CD25+Tregs into systemic MDA5 G821S mice resulted in weight gain and increased survival (Figures 7 B and C). The apoptosis of Tregs in MDA5 G821S mice was shown to be rescued by IFNAR deficiency (Figure 6) and cell therapy (Figure 7). These results indicates that type I IFN signaling is critical for inducing Treg cell death.

It is interesting to investigate Treg function in patients with type I interferonopathy driven by MDA5 and other gene mutations. Several studies have demonstrated that the decrease in activated Treg (CD25+Foxp3+), which is established in patients with SLE, was likewise observed in other interferonopathies [55,56]. Similar to SLE patients, I found that activated Treg was significantly reduced in AGS patients compared to healthy individuals. (Figure 9 E).

Steroids and JAK inhibitors are the main treatments for patients with AGS [57].Steroids can reduce inflammation by blocking inflammatory cytokines. Meanwhile, JAK inhibitors control T cell proliferation by inhibiting the JAK-STAT signaling pathway, which eventually down-regulates IL-2, IL-4, IL-6, IL-21, and IFN-r levels [58].

Moreover, JAK inhibitors control the apoptosis gene, and expression of STATs is associated with apoptosis. STAT1 promote the induction of caspases 1, 3, and links with the p53 protein. Furthermore, STAT1 activates other pro-apoptosis genes such as Fas, PUMA, and Noxa [59-61]. STAT3 inhibits the expression of anti-apoptotic proteins such as Bcl-xL, Bcl-2, and Mcl-1 [59-61]. Consistent with previous findings, JAK inhibitor treatment increased activated Tregs by preventing apoptosis of Tregs from AGS patients (Figure 9, blue). However, more studies into the underlying

mechanisms are needed to fully understand the correlation between activated Tregs and JAK inhibitors.

MDA5 signaling is known to generate type I IFN and other inflammatory cytokines, including IL-6 and TNF-α. The effect of type I IFN on Treg apoptosis has been shown to be essential; however, the role of other inflammatory cytokines in Treg apoptosis in MDA5 mutant mice requires further investigation, especially the underlying mechanisms. Moreover, a Treg-specific expression system of the MDA5 mutant will be required to further understand what will be the critical factors induced by the MDA5 primary signaling and/or secondary signaling, such as IFNAR signaling, to change Tregs into apoptosis.

In conclusion, I provide evidence that MDA5 mutant signaling on Tregs leads to apoptosis in Tregs and may trigger the onset of type I interferonopathies such as AGS. Therefore, MDA5 could be a useful therapeutic target to control the number of Treg cells and immunological responses in cancer or autoimmune diseases.

Chapter 5

Bibliography

Bibliography

[1] Romani L. Immunity to fungal infections. Nat Rev Immunol. 2011 Apr;11(4):275-88. doi: 10.1038/nri2939. Epub 2011 Mar 11. PMID: 21394104.

[2] Medzhitov R, Janeway CA Jr. Innate immunity: impact on the adaptive immune response. Curr Opin Immunol. 1997 Feb;9(1):4-9. doi: 10.1016/s0952-7915(97)80152-5. PMID: 9039775.

[3] Iwasaki A, Medzhitov R. Control of adaptive immunity by the innate immune system. Nat Immunol. 2015 Apr;16(4):343-53. doi: 10.1038/ni.3123. PMID: 25789684; PMCID: PMC4507498.

[4] Yoneyama M, Fujita T. RNA recognition and signal transduction by RIG-I-like receptors. Immunol Rev. 2009 Jan;227(1):54-65. doi: 10.1111/j.1600-065X.2008.00727.x. PMID: 19120475.

[5] Roth-Cross JK, Bender SJ, Weiss SR. Murine coronavirus mouse hepatitis virus is recognized by MDA5 and induces type I interferon in brain macrophages/microglia. J Virol. 2008 Oct;82(20):9829-38. doi: 10.1128/JVI.01199-08. Epub 2008 Jul 30. PMID: 18667505; PMCID: PMC2566260.

[6] Mogensen TH. Pathogen recognition and inflammatory signaling in innate immune defenses. Clin Microbiol Rev. 2009 Apr;22(2):240-73, Table of Contents. doi: 10.1128/CMR.00046-08. PMID: 19366914; PMCID: PMC2668232.

[7] Kawai T, Takahashi K, Sato S, Coban C, Kumar H, Kato H, Ishii KJ, Takeuchi O, Akira S. IPS-1, an adaptor triggering RIG-I- and Mda5-mediated type I interferon induction. Nat Immunol. 2005 Oct;6(10):981-8. doi: 10.1038/ni1243. Epub 2005 Aug 28. PMID: 16127453.

[8] Gitlin L, Barchet W, Gilfillan S, Cella M, Beutler B, Flavell RA, Diamond MS, Colonna M. Essential role of mda-5 in type I IFN responses to

polyriboinosinic:polyribocytidylic acid and encephalomyocarditis picornavirus. Proc Natl Acad Sci U S A. 2006 May 30;103(22):8459-64. doi: 10.1073/pnas.0603082103. Epub 2006 May 19. PMID: 16714379; PMCID: PMC1464000.

[9] Loo YM, Gale M Jr. Immune signaling by RIG-I-like receptors. Immunity. 2011 May 27;34(5):680-92. doi: 10.1016/j.immuni.2011.05.003. PMID: 21616437; PMCID: PMC3177755.

[10] Li D, Wu M. Pattern recognition receptors in health and diseases. Signal Transduct Target Ther. 2021 Aug 4;6(1):291. doi: 10.1038/s41392-021-00687-0. PMID: 34344870; PMCID: PMC8333067.

[11] Crow MK, Olferiev M, Kirou KA. Type I Interferons in Autoimmune Disease. Annu Rev Pathol. 2019 Jan 24;14:369-393. doi: 10.1146/annurev-pathol-020117-043952. Epub 2018 Oct 17. PMID: 30332560.

[12] Psarras A, Emery P, Vital EM. Type I interferon-mediated autoimmune diseases: pathogenesis, diagnosis and targeted therapy. Rheumatology (Oxford). 2017 Oct 1;56(10):1662-1675. doi: 10.1093/rheumatology/kew431. PMID: 28122959.

[13] Banchereau J, Pascual V. Type I interferon in systemic lupus erythematosus and other autoimmune diseases. Immunity. 2006 Sep;25(3):383-92. doi: 10.1016/j.immuni.2006.08.010. PMID: 16979570.

[14] Oleksy B, Mierzewska H, Tryfon J, Wypchło M, Wasilewska K, Zalewska-Miszkurka Z, Płoski R, Rydzanicz M, Szczepanik E. Aicardi-Goutières Syndrome due to a *SAMHD1* Mutation Presenting with Deep White Matter Cysts. Mol Syndromol. 2022 Feb;13(2):132-138. doi: 10.1159/000518941. Epub 2021 Nov 18. PMID: 35418820; PMCID: PMC8928195.

[15] Sase S, Takanohashi A, Vanderver A, Almad A. Astrocytes, an active player in Aicardi-Goutières syndrome. Brain Pathol. 2018 May;28(3):399-407. doi: 10.1111/bpa.12600. PMID: 29740948; PMCID: PMC8028286.

[16] Crow YJ, Manel N. Aicardi-Goutières syndrome and the type I interferonopathies. Nat Rev Immunol. 2015 Jul;15(7):429-40. doi: 10.1038/nri3850. Epub 2015 Jun 5. PMID: 26052098.

[17] Rice G, Patrick T, Parmar R, Taylor CF, Aeby A, Aicardi J, Artuch R, Montalto SA, Bacino CA, Barroso B, Baxter P, Benko WS, Bergmann C, Bertini E, Biancheri R, Blair EM, Blau N, Bonthron DT, Briggs T, Brueton LA, Brunner HG, Burke CJ, Carr IM, Carvalho DR, Chandler KE, Christen HJ, Corry PC, Cowan FM, Cox H, D'Arrigo S, Dean J, De Laet C, De Praeter C, Dery C, Ferrie CD, Flintoff K, Frints SG, Garcia-Cazorla A, Gener B, Goizet C, Goutieres F, Green AJ, Guet A, Hamel BC, Hayward BE, Heiberg A, Hennekam RC, Husson M, Jackson AP, Jayatunga R, Jiang YH, Kant SG, Kao A, King MD, Kingston HM, Klepper J, van der Knaap MS, Kornberg AJ, Kotzot D, Kratzer W, Lacombe D, Lagae L, Landrieu PG, Lanzi G, Leitch A, Lim MJ, Livingston JH, Lourenco CM, Lyall EG, Lynch SA, Lyons MJ, Marom D, McClure JP, McWilliam R, Melancon SB, Mewasingh LD, Moutard ML, Nischal KK, Ostergaard JR, Prendiville J, Rasmussen M, Rogers RC, Roland D, Rosser EM, Rostasy K, Roubertie A, Sanchis A, Schiffmann R, Scholl-Burgi S, Seal S, Shalev SA, Corcoles CS, Sinha GP, Soler D, Spiegel R, Stephenson JB, Tacke U, Tan TY, Till M, Tolmie JL, Tomlin P, Vagnarelli F, Valente EM, Van Coster RN, Van der Aa N, Vanderver A, Vles JS, Voit T, Wassmer E, Weschke B, Whiteford ML, Willemsen MA, Zankl A, Zuberi SM, Orcesi S, Fazzi E, Lebon P, Crow YJ. Clinical and molecular phenotype of Aicardi-Goutieres syndrome. Am J Hum Genet. 2007 Oct;81(4):713-25. doi: 10.1086/521373. Epub 2007 Sep 4. PMID: 17846997; PMCID: PMC2227922.

[18] Kambayashi T, Laufer TM. Atypical MHC class II-expressing antigen-presenting cells: can anything replace a dendritic cell? Nat Rev Immunol. 2014 Nov;14(11):719-30. doi: 10.1038/nri3754. Epub 2014 Oct 17. PMID: 25324123.

[19] Holling TM, Schooten E, van Den Elsen PJ. Function and regulation of MHC class II molecules in T-lymphocytes: of mice and men. Hum Immunol. 2004 Apr;65(4):282-90. doi: 10.1016/j.humimm.2004.01.005. PMID: 15120183.

[20] Kambayashi T, Laufer TM. Atypical MHC class II-expressing antigen-presenting cells: can anything replace a dendritic cell? Nat Rev Immunol. 2014 Nov;14(11):719-30. doi: 10.1038/nri3754. Epub 2014 Oct 17. PMID: 25324123.

[21] Grusby MJ, Johnson RS, Papaioannou VE, Glimcher LH. Depletion of CD4+ T cells in major histocompatibility complex class II-deficient mice. Science. 1991 Sep 20;253(5026):1417-20. doi: 10.1126/science.1910207. PMID: 1910207.

[22] Belizário JE, Brandão W, Rossato C, Peron JP. Thymic and Postthymic Regulation of Naïve CD4(+) T-Cell Lineage Fates in Humans and Mice Models. Mediators Inflamm. 2016;2016:9523628. doi: 10.1155/2016/9523628. Epub 2016 May 30. PMID: 27313405; PMCID: PMC4904118.

[23] Zhu J, Paul WE. CD4 T cells: fates, functions, and faults. Blood. 2008 Sep 1;112(5):1557-69. doi: 10.1182/blood-2008-05-078154. PMID: 18725574; PMCID: PMC2518872.

[24] Wan YY. GATA3: a master of many trades in immune regulation. Trends Immunol. 2014 Jun;35(6):233-42. doi: 10.1016/j.it.2014.04.002. Epub 2014 Apr 28. PMID: 24786134; PMCID: PMC4045638.

[25] Maverakis E, Kim K, Shimoda M, Gershwin ME, Patel F, Wilken R, Raychaudhuri S, Ruhaak LR, Lebrilla CB. Glycans in the immune system and The Altered Glycan Theory of Autoimmunity: a critical review. J Autoimmun. 2015 Feb;57:1-13. doi:

10.1016/j.jaut.2014.12.002. Epub 2015 Jan 9. PMID: 25578468; PMCID: PMC4340844.

[26] Toscano MA, Bianco GA, Ilarregui JM, Croci DO, Correale J, Hernandez JD, Zwirner NW, Poirier F, Riley EM, Baum LG, Rabinovich GA. Differential glycosylation of TH1, TH2 and TH-17 effector cells selectively regulates susceptibility to cell death. Nat Immunol. 2007 Aug;8(8):825-34. doi: 10.1038/ni1482. Epub 2007 Jun 24. PMID: 17589510.

[27] Harrington LE, Hatton RD, Mangan PR, Turner H, Murphy TL, Murphy KM, Weaver CT. Interleukin 17-producing CD4+ effector T cells develop via a lineage distinct from the T helper type 1 and 2 lineages. Nat Immunol. 2005 Nov;6(11):1123-32. doi: 10.1038/ni1254. Epub 2005 Oct 2. PMID: 16200070.

[28] Hang S, Paik D, Yao L, Kim E, Trinath J, Lu J, Ha S, Nelson BN, Kelly SP, Wu L, Zheng Y, Longman RS, Rastinejad F, Devlin AS, Krout MR, Fischbach MA, Littman DR, Huh JR. Bile acid metabolites control TH17 and Treg cell differentiation. Nature. 2019 Dec;576(7785):143-148. doi: 10.1038/s41586-019-1785-z. Epub 2019 Nov 27. Erratum in: Nature. 2020 Mar;579(7798):E7. PMID: 31776512; PMCID: PMC6949019.

[29] Hirota K, Duarte JH, Veldhoen M, Hornsby E, Li Y, Cua DJ, Ahlfors H, Wilhelm C, Tolaini M, Menzel U, Garefalaki A, Potocnik AJ, Stockinger B. Fate mapping of IL-17-producing T cells in inflammatory responses. Nat Immunol. 2011 Mar;12(3):255-63. doi: 10.1038/ni.1993. Epub 2011 Jan 30. PMID: 21278737; PMCID: PMC3040235.

[30] Nakayamada S, Takahashi H, Kanno Y, O'Shea JJ. Helper T cell diversity and plasticity. Curr Opin Immunol. 2012 Jun;24(3):297-302. doi: 10.1016/j.coi.2012.01.014. Epub 2012 Feb 15. PMID: 22341735; PMCID: PMC3383341.

[31] Curiel TJ. Tregs and rethinking cancer immunotherapy. J Clin Invest. 2007 May;117(5):1167-74. doi: 10.1172/JCI31202. PMID: 17476346; PMCID: PMC1857250.

[32] S. Sakaguchi, T. Yamaguchi, T. Nomura, M. Ono, Regulatory T cells and immune tolerance, cell. (2008) May 30;133(5):775-87,

[33] Sakaguchi S, Ono M, Setoguchi R, Yagi H, Hori S, Fehervari Z, Shimizu J, Takahashi T, Nomura T. Foxp3+ CD25+ CD4+ natural regulatory T cells in dominant self-tolerance and autoimmune disease. Immunol Rev. 2006 Aug;212:8-27. doi: 10.1111/j.0105-2896.2006.00427.x. PMID: 16903903.

[34] Read S, Greenwald R, Izcue A, Robinson N, Mandelbrot D, Francisco L, Sharpe AH, Powrie F. Blockade of CTLA-4 on CD4+CD25+ regulatory T cells abrogates their function in vivo. J Immunol. 2006 Oct 1;177(7):4376-83. doi: 10.4049/jimmunol.177.7.4376. PMID: 16982872; PMCID: PMC6108417.

[35] Guarda G, Dostert C, Staehli F, Cabalzar K, Castillo R, Tardivel A, Schneider P, Tschopp J. T cells dampen innate immune responses through inhibition of NLRP1 and NLRP3 inflammasomes. Nature. 2009 Jul 9;460(7252):269-73. doi: 10.1038/nature08100. Epub 2009 Jun 3. PMID: 19494813.

[36] Coutinho A, Caramalho I, Seixas E, Demengeot J. Thymic commitment of regulatory T cells is a pathway of TCR-dependent selection that isolates repertoires undergoing positive or negative selection. Curr Top Microbiol Immunol. 2005;293:43-71. doi: 10.1007/3-540-27702-1_3. PMID: 15981475.

[37] Brunkow ME, Jeffery EW, Hjerrild KA, Paeper B, Clark LB, Yasayko SA, Wilkinson JE, Galas D, Ziegler SF, Ramsdell F. Disruption of a new forkhead/winged-helix protein, scurfin, results in the fatal lymphoproliferative disorder of the scurfy mouse. Nat Genet. 2001 Jan;27(1):68-73. doi: 10.1038/83784. PMID: 11138001.

[38] Wildin RS, Ramsdell F, Peake J, Faravelli F, Casanova JL, Buist N, Levy-Lahad E, Mazzella M, Goulet O, Perroni L, Bricarelli FD, Byrne G, McEuen M, Proll S, Appleby M, Brunkow ME. X-linked neonatal diabetes mellitus, enteropathy and endocrinopathy syndrome is the human equivalent of mouse scurfy. Nat Genet. 2001 Jan;27(1):18-20. doi: 10.1038/83707. PMID: 11137992.

[39] A. Gangaplara, C. Martens, E. Dahlstrom, A. Metidji, AS. Gokhale , DD. Glass, M. Lopez-Ocasio, R. Baur, K. Kanakabandi, SF. Porcella, EM. Shevach. Type I interferon signaling attenuates regulatory T cell function in viral infection and in the tumor microenvironment. PLoS Pathog. 2018 Apr 19;14(4):e1006985.

[40] S. Srivastava, L.K. Koch, D.J. Campbell, IFNαR signaling in effector but not regulatory T cells is required for immune dysregulation during type I IFN-dependent inflammatory disease. J Immunol. 2014 Sep 15;193(6):2733-42.

[41] M. Funabiki, H. Kato, Y. Miyachi, H. Toki, H. Motegi, M. Inoue, O. Minowa, A. Yoshida, K. Deguchi, H. Sato, S. Ito, T. Shiroishi, K. Takeyasu, T. Noda, T. Fujita, Autoimmune Disorders Associated with Gain of Function of the Intracellular Sensor MDA5, Immunity. 40 (2014) 199–212.

[42] H. Onizawa, H. Kato, H. Kimura, T. Kudo, N. Soda, S. Shimizu, M. Funabiki, Y. Yagi, Y. Nakamoto, J. Priller, R. Nishikomori, T. Heike, N. Yan, T. Tsujimura, T. Mimori and T. Fujita, Aicardi–Goutières syndrome-like encephalitis in mutant mice with constitutively active MDA5, International Immunology, 33(2020) 225–240

[43] N. Soda, N. Sakai, Kato, M. Takami, T. Fujita, Singleton-Merten Syndrome–like Skeletal Abnormalities in Mice with Constitutively Activated MDA5, J Immunol. 2019 Sep 1;203(5):1356-1368.

[44] Corthay A. How do regulatory T cells work? Scand J Immunol. 2009 Oct;70(4):326-36. doi: 10.1111/j.1365-3083.2009.02308.x. PMID: 19751267; PMCID: PMC2784904.

[45] AM. Thornton, PE. Korty, DQ.Tran, EA.Wohlfert, PE. Murray, Y. Belkaid, EM.Shevach. Expression of Helios, an Ikaros transcription factor family member, differentiates thymic-derived from peripherally induced Foxp3+ T regulatory cells. J Immunol. 2010 Apr 1;184(7):3433-41.

[46] Kühn R, Torres RM. Cre/loxP recombination system and gene targeting. Methods Mol Biol. 2002;180:175-204. doi: 10.1385/1-59259-178-7:175. PMID: 11873650.

[47] Raimbourg Q, Daugas É. Atteintes rénales du lupus [Lupus nephritis]. Nephrol Ther. 2019 Jun;15(3):174-189. French. doi: 10.1016/j.nephro.2018.11.003. Epub 2019 Feb 7. PMID: 30738732.

[48] Wildin RS, Ramsdell F, Peake J, Faravelli F, Casanova JL, Buist N, Levy-Lahad E, Mazzella M, Goulet O, Perroni L, Bricarelli FD, Byrne G, McEuen M, Proll S, Appleby M, Brunkow ME. X-linked neonatal diabetes mellitus, enteropathy and endocrinopathy syndrome is the human equivalent of mouse scurfy. Nat Genet. 2001 Jan;27(1):18-20. doi: 10.1038/83707. PMID: 11137992.

[49] Markram H, Toledo-Rodriguez M, Wang Y, Gupta A, Silberberg G, Wu C. Interneurons of the neocortical inhibitory system. Nat Rev Neurosci. 2004 Oct;5(10):793-807. doi: 10.1038/nrn1519. PMID: 15378039.

[50] Humrich JY, Morbach H, Undeutsch R, Enghard P, Rosenberger S, Weigert O, Kloke L, Heimann J, Gaber T, Brandenburg S, Scheffold A, Huehn J, Radbruch A, Burmester GR, Riemekasten G. Homeostatic imbalance of regulatory and effector T cells due to IL-2 deprivation amplifies murine lupus. Proc Natl Acad Sci U S A. 2010

Jan 5;107(1):204-9. doi: 10.1073/pnas.0903158107. Epub 2009 Dec 14. PMID: 20018660; PMCID: PMC2806746.

[51] Asano M, Toda M, Sakaguchi N, Sakaguchi S. Autoimmune disease as a consequence of developmental abnormality of a T cell subpopulation. J Exp Med. 1996 Aug 1;184(2):387-96. doi: 10.1084/jem.184.2.387. PMID: 8760792; PMCID: PMC2192701.

[52] Miyara M, Yoshioka Y, Kitoh A, Shima T, Wing K, Niwa A, Parizot C, Taflin C, Heike T, Valeyre D, Mathian A, Nakahata T, Yamaguchi T, Nomura T, Ono M, Amoura Z, Gorochov G, Sakaguchi S. Functional delineation and differentiation dynamics of human CD4+ T cells expressing the FoxP3 transcription factor. Immunity. 2009 Jun 19;30(6):899-911. doi: 10.1016/j.immuni.2009.03.019. Epub 2009 May 21. PMID: 19464196.

[53] Sohn SY, Song YW, Yeo YK, Kim YK, Jang GY, Woo CW, Lee JH, Lee KC. Alteration of CD4CD25Foxp3 T cell level in Kawasaki disease. Korean J Pediatr. 2011 Apr;54(4):157-62. doi: 10.3345/kjp.2011.54.4.157. Epub 2011 Apr 30. PMID: 21738549; PMCID: PMC3127149.

[54] Tsai MS, Lee JL, Chang YJ, Hwang SM. Isolation of human multipotent mesenchymal stem cells from second-trimester amniotic fluid using a novel two-stage culture protocol. Hum Reprod. 2004 Jun;19(6):1450-6. doi: 10.1093/humrep/deh279. Epub 2004 Apr 22. PMID: 15105397.

[55] Li W, Deng C, Yang H, Wang G. The Regulatory T Cell in Active Systemic Lupus Erythematosus Patients: A Systemic Review and Meta-Analysis. Front Immunol. 2019 Feb 18;10:159. doi: 10.3389/fimmu.2019.00159. PMID: 30833946; PMCID: PMC6387904.

[56] Mizui M, Tsokos GC. Targeting Regulatory T Cells to Treat Patients With Systemic Lupus Erythematosus. Front Immunol. 2018 Apr 17;9:786. doi: 10.3389/fimmu.2018.00786. PMID: 29755456; PMCID: PMC5932391.

[57] Vanderver A, Adang L, Gavazzi F, McDonald K, Helman G, Frank DB, Jaffe N, Yum SW, Collins A, Keller SR, Lebon P, Meritet JF, Rhee J, Takanohashi A, Armangue T, Ulrick N, Sherbini O, Koh J, Peer K, Besnier C, Scher C, Boyle K, Dubbs H, Kramer-Golinkoff J, Pizzino A, Woidill S, Shults J. Janus Kinase Inhibition in the Aicardi-Goutières Syndrome. N Engl J Med. 2020 Sep 3;383(10):986-989. doi: 10.1056/NEJMc2001362. PMID: 32877590; PMCID: PMC7495410.

[58] Kubo S, Nakayamada S, Sakata K, Kitanaga Y, Ma X, Lee S, Ishii A, Yamagata K, Nakano K, Tanaka Y. Janus Kinase Inhibitor Baricitinib Modulates Human Innate and Adaptive Immune System. Front Immunol. 2018 Jun 28;9:1510. doi: 10.3389/fimmu.2018.01510. PMID: 30002661; PMCID: PMC6031708.

[59] Hu X, Li J, Fu M, Zhao X, Wang W. The JAK/STAT signaling pathway: from bench to clinic. Signal Transduct Target Ther. 2021 Nov 26;6(1):402. doi: 10.1038/s41392-021-00791-1. PMID: 34824210; PMCID: PMC8617206.

[60] Seif F, Khoshmirsafa M, Aazami H, Mohsenzadegan M, Sedighi G, Bahar M. The role of JAK-STAT signaling pathway and its regulators in the fate of T helper cells. Cell Commun Signal. 2017 Jun 21;15(1):23. doi: 10.1186/s12964-017-0177-y. PMID: 28637459; PMCID: PMC5480189.

[61] Bousoik E, Montazeri Aliabadi H. "Do We Know Jack" About JAK? A Closer Look at JAK/STAT Signaling Pathway. Front Oncol. 2018 Jul 31;8:287. doi: 10.3389/fonc.2018.00287. PMID: 30109213; PMCID: PMC6079274.

Chapter 6

Acknowledgments

I would like to express my sincere gratitude to all those who allowed me to complete this dissertation. Special thanks are due to my supervisor Prof. Takashi Fujita, who kindly mentored and supported me through my Ph.D. studies. It has been an honor for me to work in the Fujita lab. And I would also like to acknowledge with much appreciation the dedicated support and guidance of Prof. Hiroki Kato. His insight and knowledge steered me through this research.

I also thank Dr. Junji Uehori, Prof. Yasutaka Okabe, and Dr. Kazuya Shimura. The completion of my dissertation could not have been accomplished without their kind fellowship and support.

Finally, as always, my lovely family provided all sorts of tangible and intangible support. My heartfelt thanks to my family.

This work was supported by independent grants from the Japan Science and Technology Agency, from the Ministry of Education, Culture, Sports, Science and Technology of Japan (innovative areas, infection competency, 24115004), Japan Agency for Medical Research and Development under grants JP17ek0109100h00 03 and JP18ek0109387h0001, The Kato Memorial Trust for Nambyo Research, and the Japan Society for the Promotion of Science Core to Core Program. This work is also funded by the Deutsche Forschungsgemeinschaft (German Research Foundation) under Germany's Excellence Strategy – EXC2151 – 390873048 and TRR237.

This thesis is based on material contained in the following scholarly paper:

Attenuation of regulatory T cell function by type I IFN signaling in an MDA5 gain-of-function mutant mouse model

Sumin Lee, Keiji Hirota, Verena Schuette, Takashi Fujita, Hiroki Kato

Biochem Biophys Res Commun 2022 Nov 12;629:171-175.

doi: 10.1016/j.bbrc.2022.09.017. Epub 2022 Sep 7.